Selective encapsulation and extraction of hydrogenphosphate by a hydrogen bond donor tripodal receptor

Sandeep Kumar Dey,*[a] Archana,[a] Sybil Pereira,[a] Sarvesh S. Harmalkar,[a] Shashank N. Mhaldar,[a] Vivekanand V. Gobre,[a] and Christoph Janiak[b]

[a]*School of Chemical Sciences, Goa University, Taleigao Plateau, Goa 403206, India.*
*E*mail: sandeepdey@unigoa.ac.in Phone: +91-7387633550
[b]*Institute for Inorganic and Structural Chemistry, Heinrich-Heine University Dusseldorf, 40225 Dusseldorf, Germany.* Email: janiak@uni-duesseldorf.de Phone: +49-8669609302

Contents

1. Materials and experimental methods

All reagents and solvents were obtained from commercial sources and used as received without further purification. Tris(2-aminoethyl) amine (Tren), 4-nitrophenyl isocyanate, 4-nitrobenzoyl chloride and all quaternary ammonium salts were purchased from Sigma-Aldrich or TCI Chemicals. Solvents (analytical grade) for synthesis and crystallization experiments were purchased from Merck, India, and used without further purification.

^{1}H and ^{31}P NMR spectra were recorded on a Bruker Advance FT-400 MHz instrument and chemical shifts were recorded in parts per million (ppm) on the scale using tetramethyl silane or residual solvent peak as a reference and ^{13}C spectra were obtained at 100 MHz at 298 K. The FT-IR spectra of dried samples were recorded on a Perkin-Elmer FT-IR spectrometer with KBr in the range 4000–450 cm^{-1}. Powder X-ray diffraction patterns of dried crystalline powder were recorded using a Bruker-D8 Advance X-ray diffractometer with Cu-*K*α radiation at λ = 0.15418 nm.

2. Synthesis and characterization

S2a. Synthesis and characterization of tris(4-amino-N-ethylbenzamide)amine (**AL**)

Tris(4-amino-N-ethylbenzamide)amine (**AL**) was synthesized by reduction of its nitro analogue (Tris(4-nitro-N-ethylbenzamide)amine**, NL**) which was synthesized by modification of the reported literature procedure (Scheme S1). **NL** was synthesized by the reaction of tris(2-aminoethyl)amine, (Tren) with 4-nitrobenzoyl chloride in 1 : 3.5 molar ratio at room temperature in dry chloroform. In a 100 mL flat bottom flask, 0.73 mL (5 mmol) of tris(2-aminoethyl)amine was dissolved in 25 mL of chloroform and 3.5 g of 4-nitrobenzoyl chloride (17.5 mmol) was added in portions into the above solution with constant stirring at room temperature. The reaction mixture was allowed to stir overnight at room temperature followed by the addition of 3 ml (excess) triethylamine and stirred for another 1 hrs. Reaction of tren with 4-nitrobenzoyl chloride generates HCl in the reaction medium, which eventually protonate the tertiary nitrogen of the formed **NL**. Triethylamine was added to basify the reaction mixture so that **NL** can be obtained in its neutral form. The precipitate obtained was then filtered, collected in a 250 ml flat bottom flask and washed with 50 ml of methanol in the presence of 1 ml of triethylamine under stirring. The compound was finally filtered again and washed with another 50 ml of methanol over the filter paper to ensure its purity for subsequent reduction reaction.

In a 250 ml flat bottom flask, 1 g of **NL** was dispersed in 100 ml of ethanol and 100 mg of Pd/C and 1 ml of hydrazine hydrate was added in to the flask. The reaction mixture was then refluxed overnight at about 80 ˚C and filtered to remove the heterogeneous Pd/C catalyst. The filtrate was then allowed to evaporate in a beaker at room temperature when colorless crystals of **AL** were obtained in quantitative yield within 2 days. The crystals were collected by decantation/filtration and washed with 10 ml of ethanol to ensure its purity for spectroscopy analysis. The compound was characterized by NMR and FT-IR spectroscopy.

Isolated yield of **AL**: 610 mg (percentage yield 71%). The compound is highly soluble in dimethylformamide, and dimethyl sulfoxide, soluble in methanol/ethanol on heating, and insoluble in tetrahydrofuran, chloroform and acetonitrile.

Characterization of **AL**: ^{1}H-NMR (400 MHz, DMSO-d_6) chemical shift in δ ppm: 2.50 (DMSO-CH_3), 2.64 (t, 6x$N\mathbf{CH_2}$), 3.30 (t, 6x$NCH_2\mathbf{CH_2}$), 3.37 (HOD), 5.56 (s, 3x$\mathbf{NH_2}$), 6.50 (d, 6xCH), 7.55 (d, 6xCH), 7.94 (t, 3x**NH**).

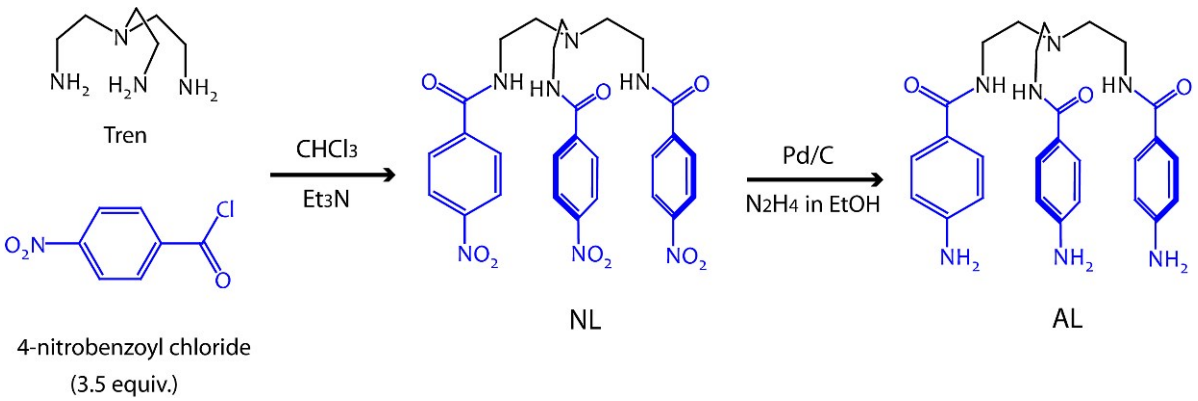

Scheme S1 Synthesis of **AL** from tris(2-aminoethylamine) and 4-nitrobenzoyl chloride.

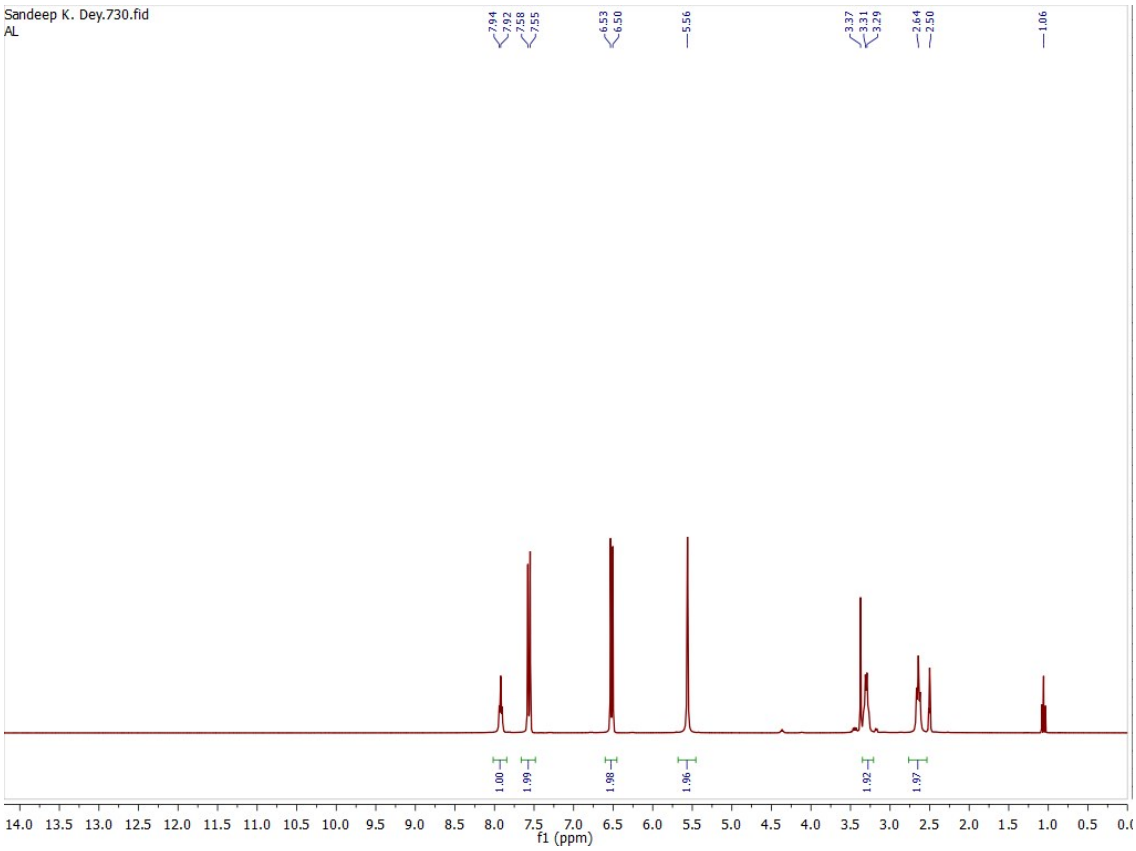

Fig. S1 ^{1}H-NMR spectrum of **AL** in DMSO-d_6.

S2b. Synthesis and characterization of tripodal urea-based receptor (AUL)

AUL was synthesized by the reaction of AL with 4-nitrophenylisocyante in a 1:3.2 molar ratio at room temperature (Scheme S2). In a 50 mL flat bottom flask, 500 mg of **AL** (1 mmol) was dissolved in 10 mL of DMSO and 0.520 g of 4-nitrophenylisocyante (3.2 mmol) was added in portions, into the above solution mixture and was allowed to stir overnight. The solution was then filtered and allowed to evaporate at room temperature in a 25 ml beaker for crystallization. Pale yellow crystals of AUL were formed in quantitative yield within a week. The crystals were collected by filtration and washed with 30 mL methanol (3 x 10 mL) to ensure its purity for spectroscopic analysis. The compound was characterized by NMR and FT-IR spectroscopy. Isolated yield of **AUL**: 650 mg (percentage yield 65%). The compound is highly soluble in dimethylformamide, and dimethyl sulfoxide, and insoluble in tetrahydrofuran, chloroform and acetonitrile and methanol/ethanol.

Characterization of **AUL**: ^{1}H-NMR (400 MHz, DMSO-d_6) chemical shift in δ ppm: 2.50 (DMSO-CH_3), 2.72 (t, 6xN$\mathbf{CH_2}$), 3.38 (6xNCH$_2\mathbf{CH_2}$ + DOH), 7.50 (d, 6xCH), 7.64 (d, 6xCH), 7.75 (d, 6xCH), 8.11 (d, 6xCH), 8.23 (s, 3x Amide-**NH**), 9.10 (s, 3x Urea-**NH**), 9.46 (s, 3x Urea-**NH**).

^{13}C-NMR (100 MHz, DMSO-d_6) chemical shift in δ ppm: 37.60 (3xCH_2), 39.50 (DMSO-CH_3), 53.38 (3xCH_2), 117.53 (6xCH), 117.58 (6xCH), 125.08 (6xCH), 128.12 (6xCH), 128.20 (3xCH), 141.08 (3xCH), 141.66 (3xCH), 146.12 (3xCH), 151.73 (3xC=O), 165.87 (3xC=O).

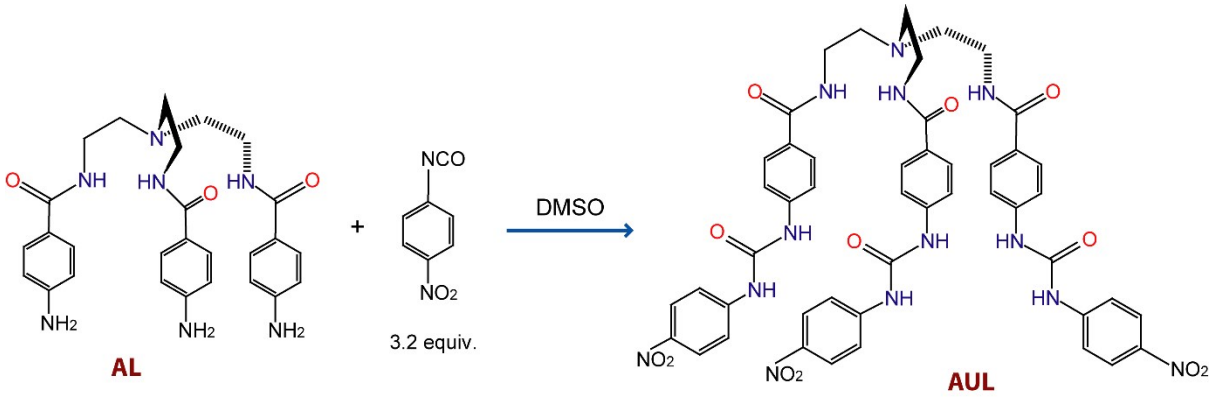

Scheme S2 Synthesis of **AUL** from tris(4-amino-N-ethylbenzamide)amine (**AL**) and 4-nitrophenyl isocyanate in DMSO.

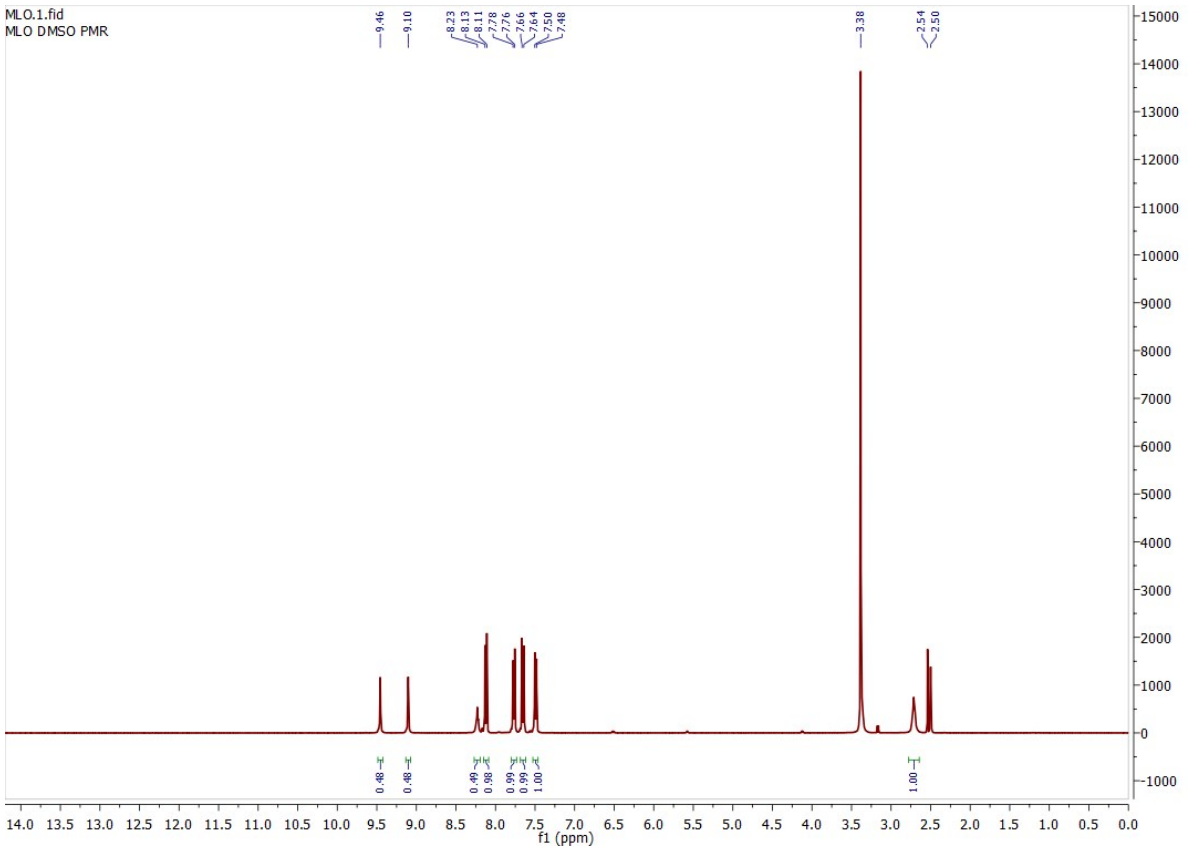

Fig. S2 ^{1}H-NMR spectrum of **AUL** in DMSO-d_6.

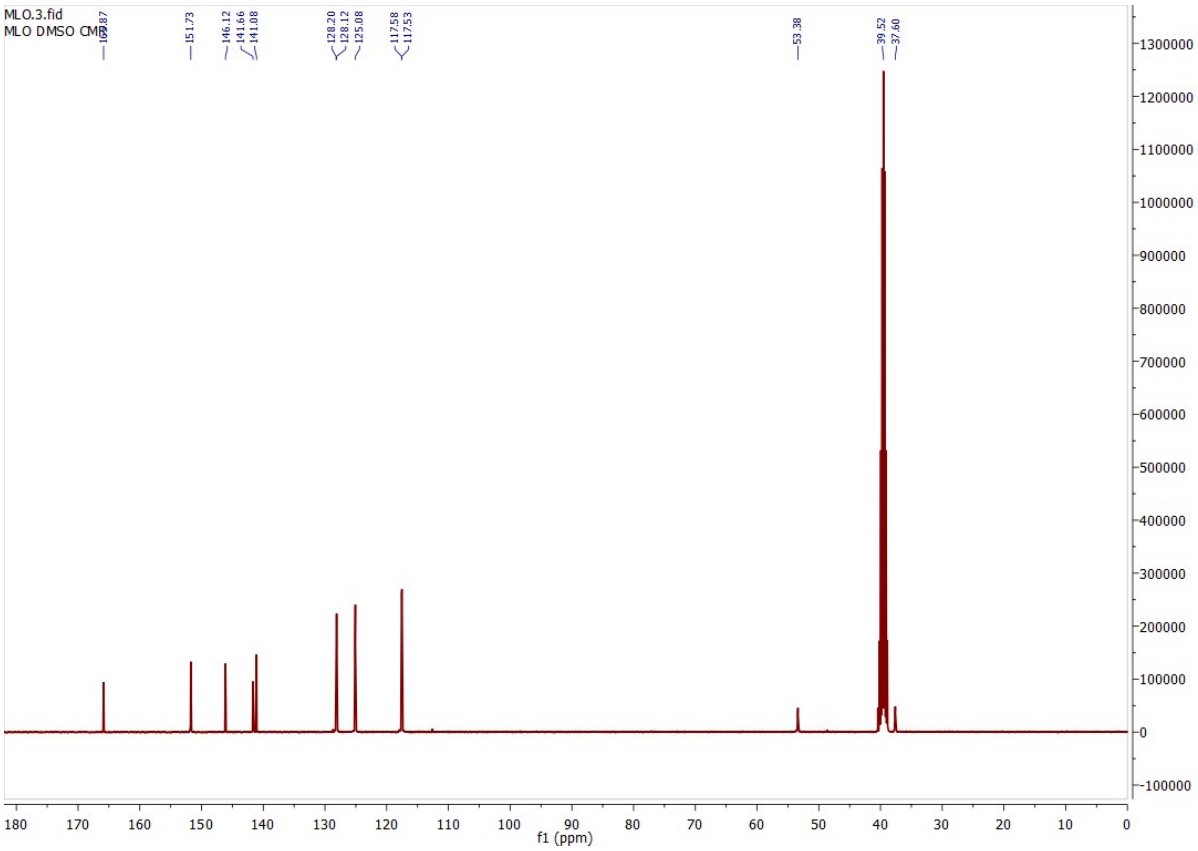

Fig. S3 ^{13}C-NMR spectrum of **AUL** in DMSO-d_6.

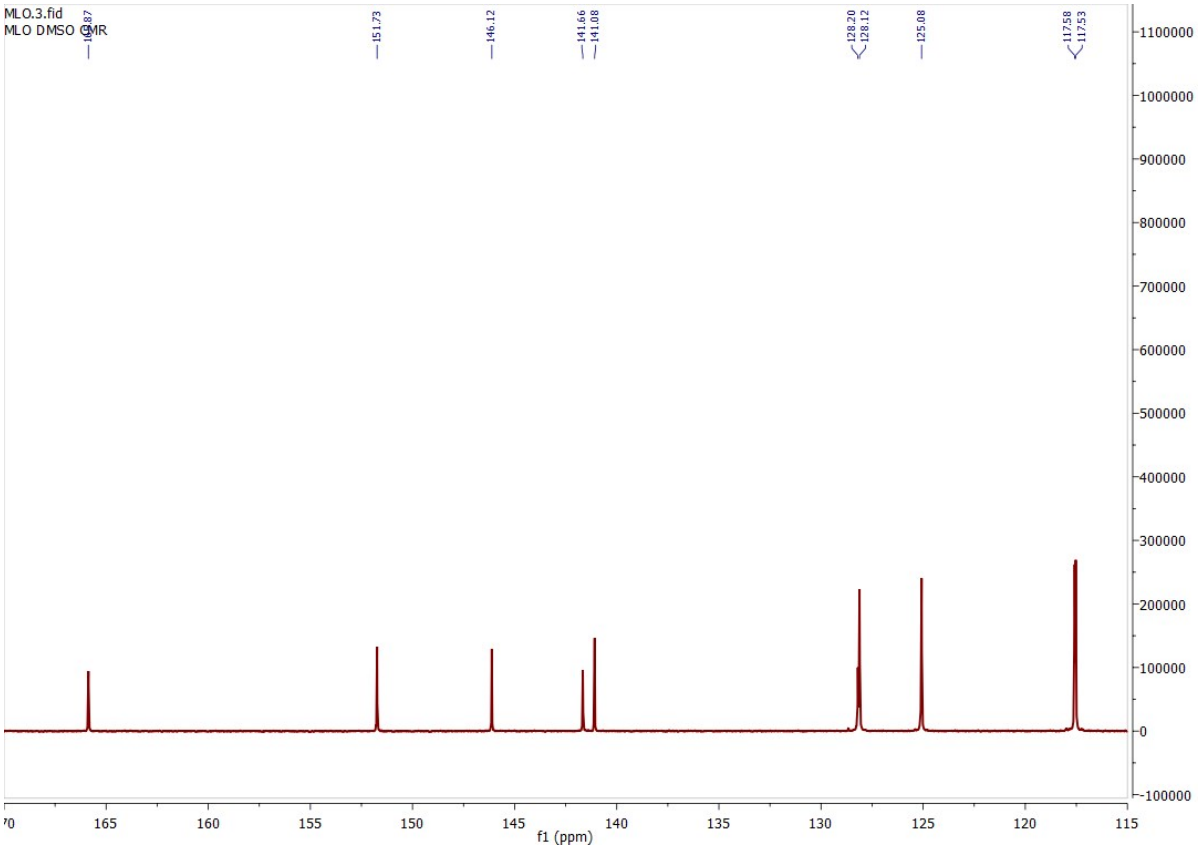

Fig. S4 ^{13}C-NMR spectrum (aromatic region) of **AUL** in DMSO-d_6.

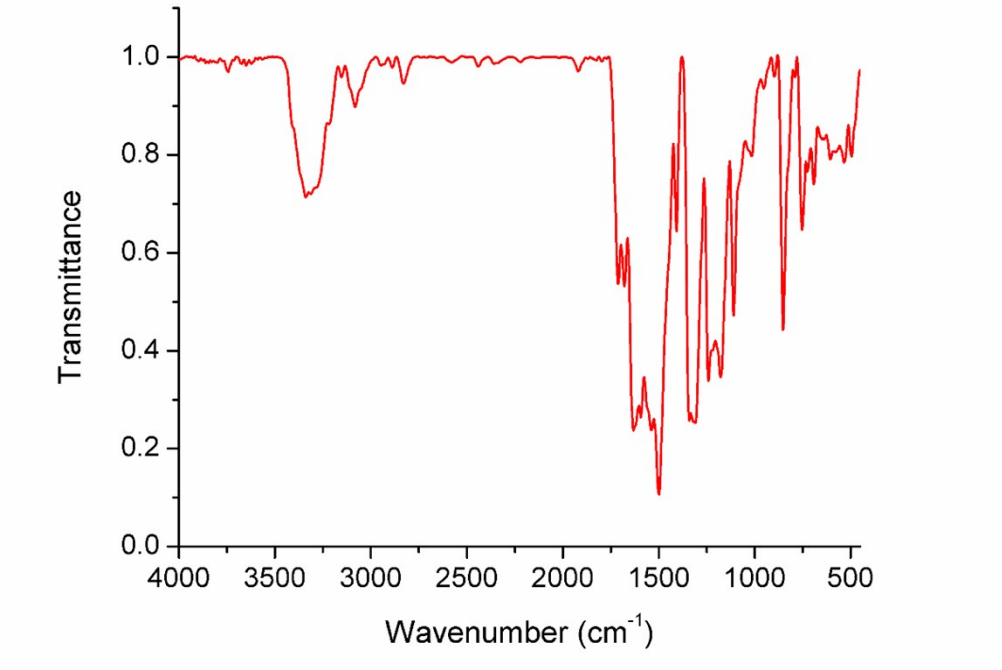

Fig. S5 FT-IR spectrum (KBr) of tripodal urea receptor **AUL**.

S2c. Synthesis and characterization of tripodal amide-based receptor (AAL)

AAL was synthesized by the reaction of **AL** with 4-nitrobenzoyl chloride, in a 1:3.5 molar ratio at room temperature. In a 250 mL flat bottom flask, 500 mg of **AL** (1 mmol) was dissolved in a tetrahydrofuran-ethanol binary solvent mixture in 8:2 (v/v) ratio (65 mL THF and 15 mL ethanol) in the presence of tetrabutylammonium chloride (2 equiv.). On complete dissolution, 550 mg of 4-nitrobenzoyl chloride (3.5 mmol) was added in small portions to the above solution mixture. The reaction mixture was stirred overnight, followed by the addition of 3 mL (excess) triethylamine and stirred for another 1 hour. The precipitate obtained was then filtered, dried and collected in a 250 mL flask and washed with 50 mL methanol in the presence of 1 mL triethylamine under stirring. The compound was then filtered again and washed with 50 mL of methanol over the filter paper to ensure its purity for subsequent analysis. The compound was characterized by NMR and FT-IR spectroscopy.

The reason for the choice of binary THF-EtOH solvent mixture for the synthesis of AAL was due to the fact that DMSO and DMF, in which **AL** is readily soluble, instead of acting as a solvent, will react with 4-nitrobenzoyl chloride to give an undesired product. Tetrabutylammonium chloride was added to partially solubilize **AL** in THF (otherwise **AL** is not soluble in THF) and addition of ethanol resulted in complete solubilisation of **AL**.

Isolated yield of **AAL**: 520 mg (percentage yield 55%). The compound is soluble in dimethylformamide, and dimethyl sulfoxide, and insoluble in tetrahydrofuran, chloroform and acetonitrile and methanol/ethanol.

^{1}H-NMR (400 MHz, DMSO-d_6) chemical shift in δ ppm: 2.50 (DMSO-CH_3), 2.74 (s, 6x$\mathbf{NCH_2}$), 3.41 (s, 6x$NCH_2\mathbf{CH_2}$), 3.39 (HOD), 7.82 (s, 12x**CH**), 8.15 (d, 6x**CH**), 8.32 (d, 6x**CH** + 3x**NH**), 10.68 (s, 3x**NH**).

^{13}C-NMR (100 MHz, DMSO-d_6) chemical shift in δ ppm: 37.56 (3xCH_2), 39.50 (DMSO-CH_3), 53.23 (3xCH_2), 119.60 (6xCH), 123.44 (6xCH), 127.82 (6xCH), 129.24 (6xCH), 129.84 (3xCH), 140.26 (3xCH), 141.15 (3xCH), 149.13 (3xCH), 163.99 (3xC=O), 165.76 (3xC=O).

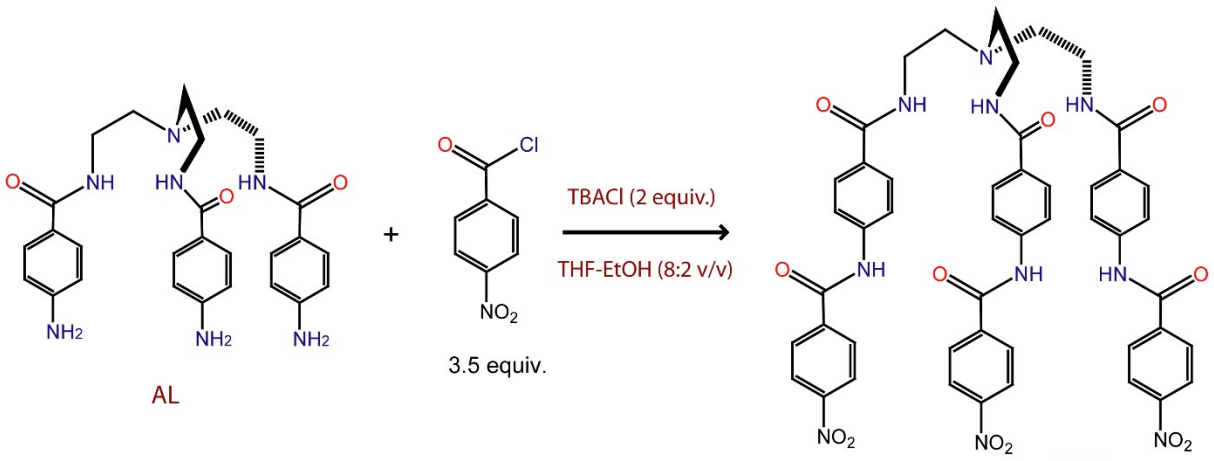

Scheme S3 Synthesis of **AAL** from **AL** and 4-nitrobenzoyl chloride.

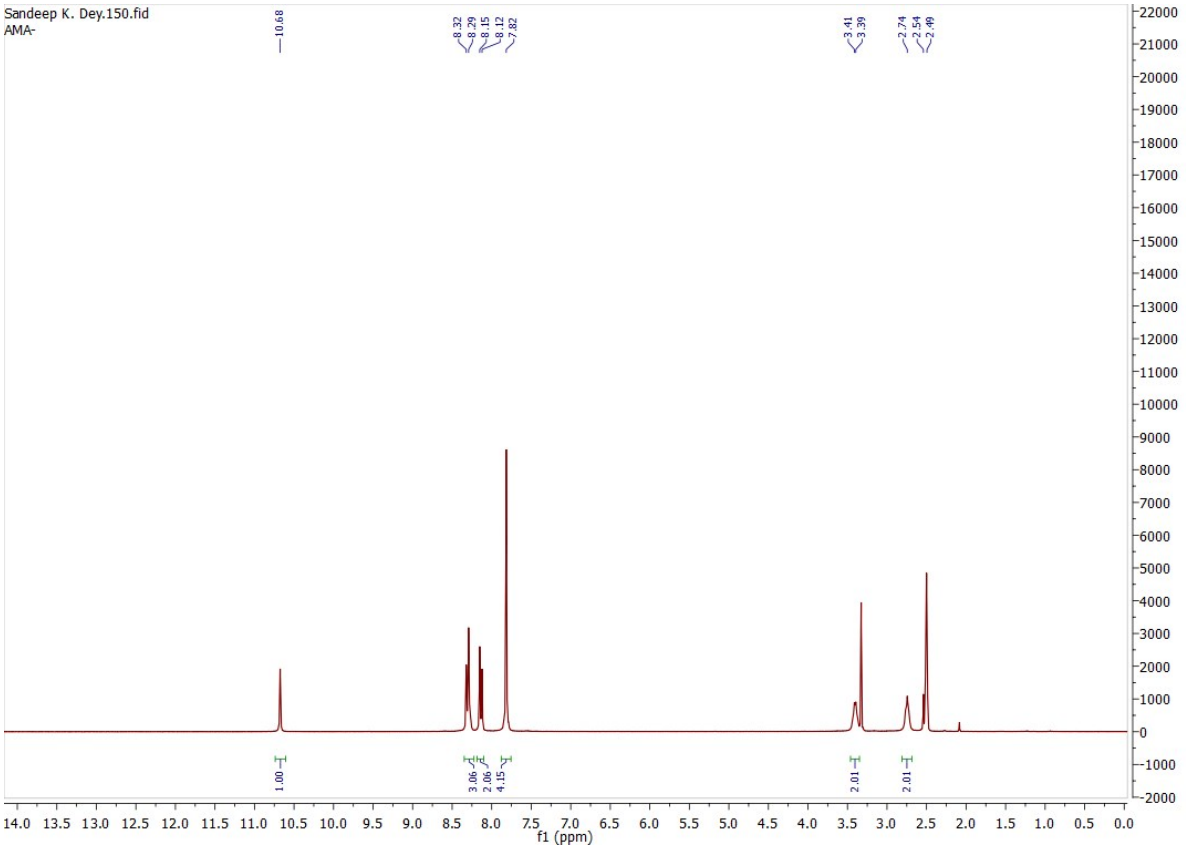

Fig. S6 ^{1}H-NMR spectrum of **AAL** in DMSO-d_6.

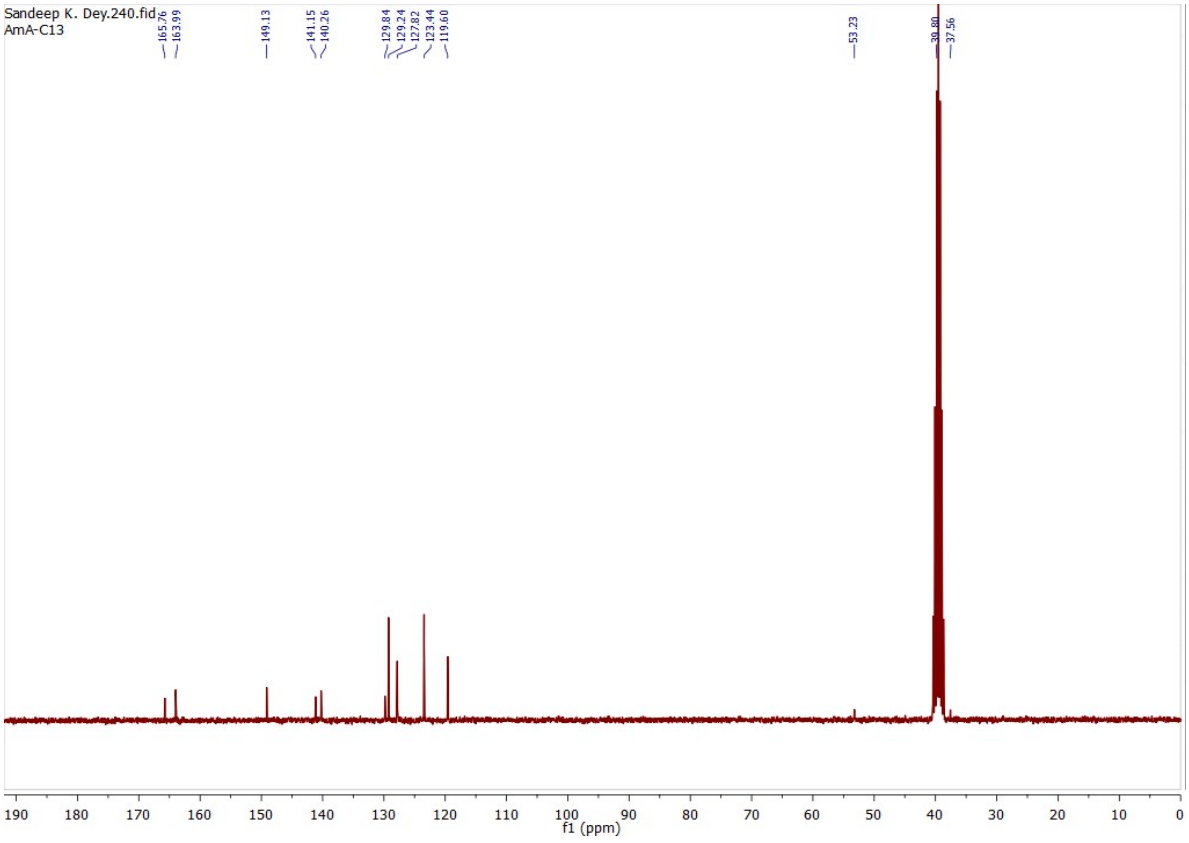

Fig. S7 ^{13}C-NMR spectrum of **AAL** in DMSO-d_6.

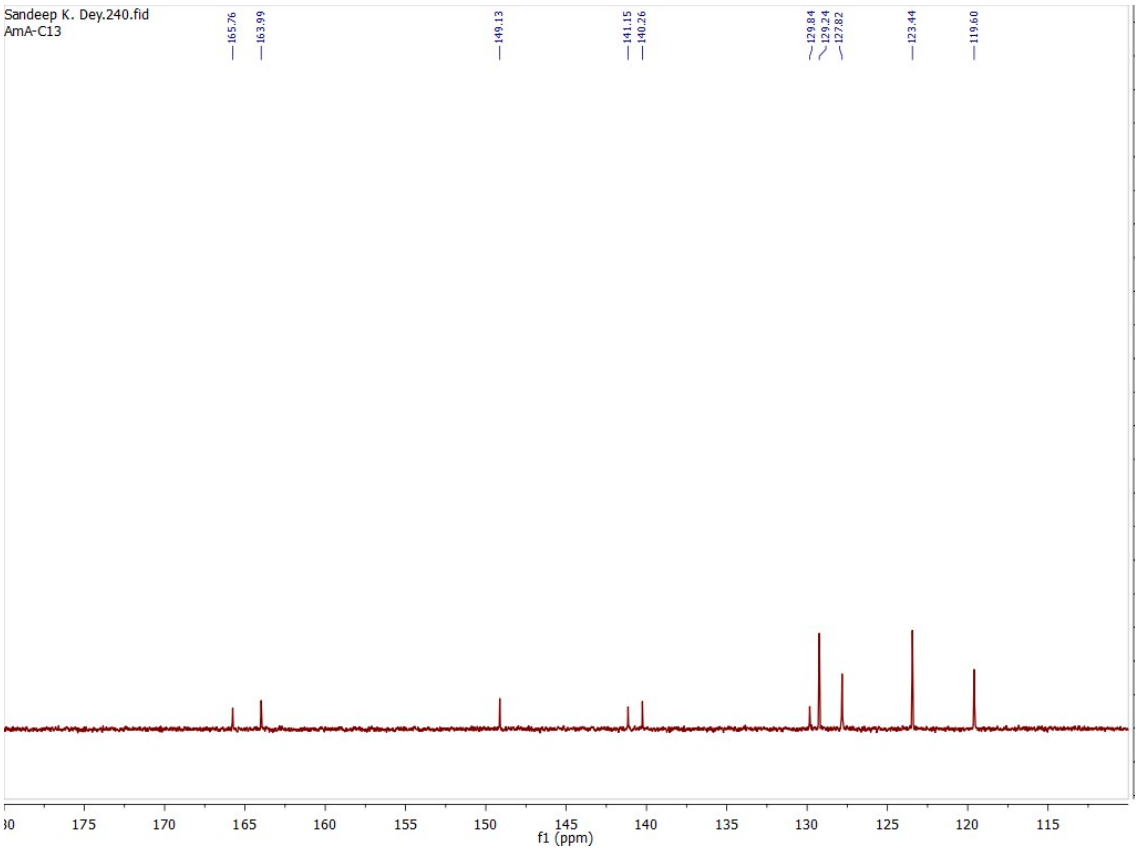

Fig. S8 Aromatic region of ^{13}C-NMR spectrum (110-180 ppm) of **AAL** in DMSO-d_6.

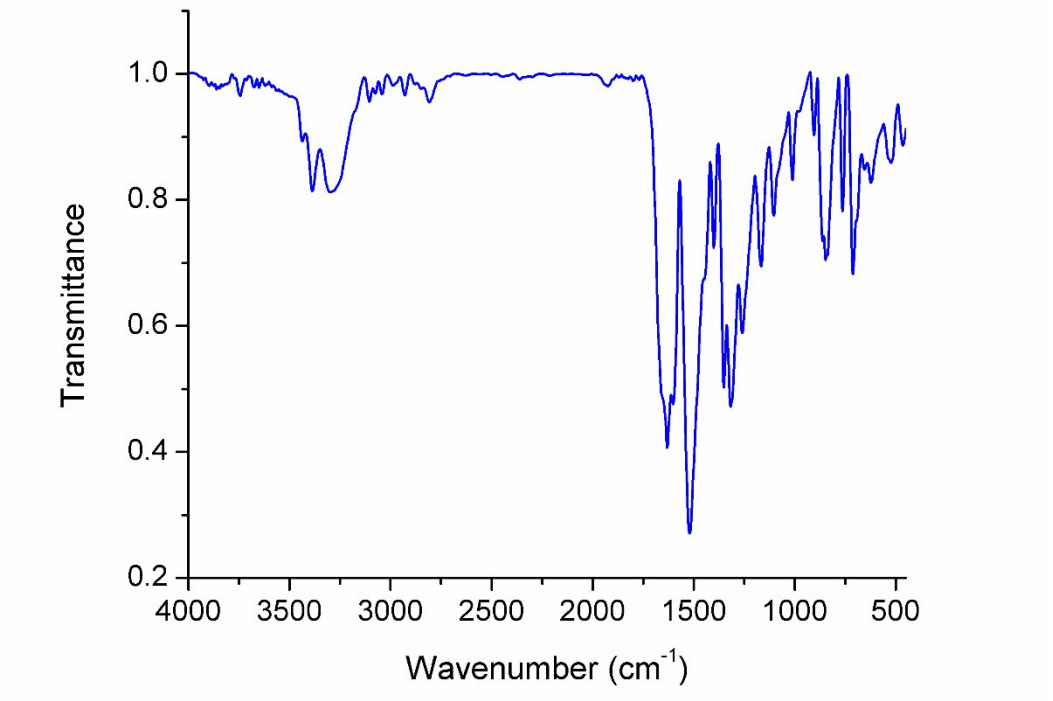

Fig. S9 FT-IR spectrum (KBr) of tripodal amide receptor **AAL**.

3. ^{1}H-NMR spectra of AUL in the presence of quaternary ammonium (n-Bu_4N^+/ Et_4N^+) salts (F^-, Cl^-, Br^-, Br_3^-, CN^-, CH_3COO^-, NO_3^-, $H_2PO_4^-$ and HSO_4^-) in DMSO-d_6.

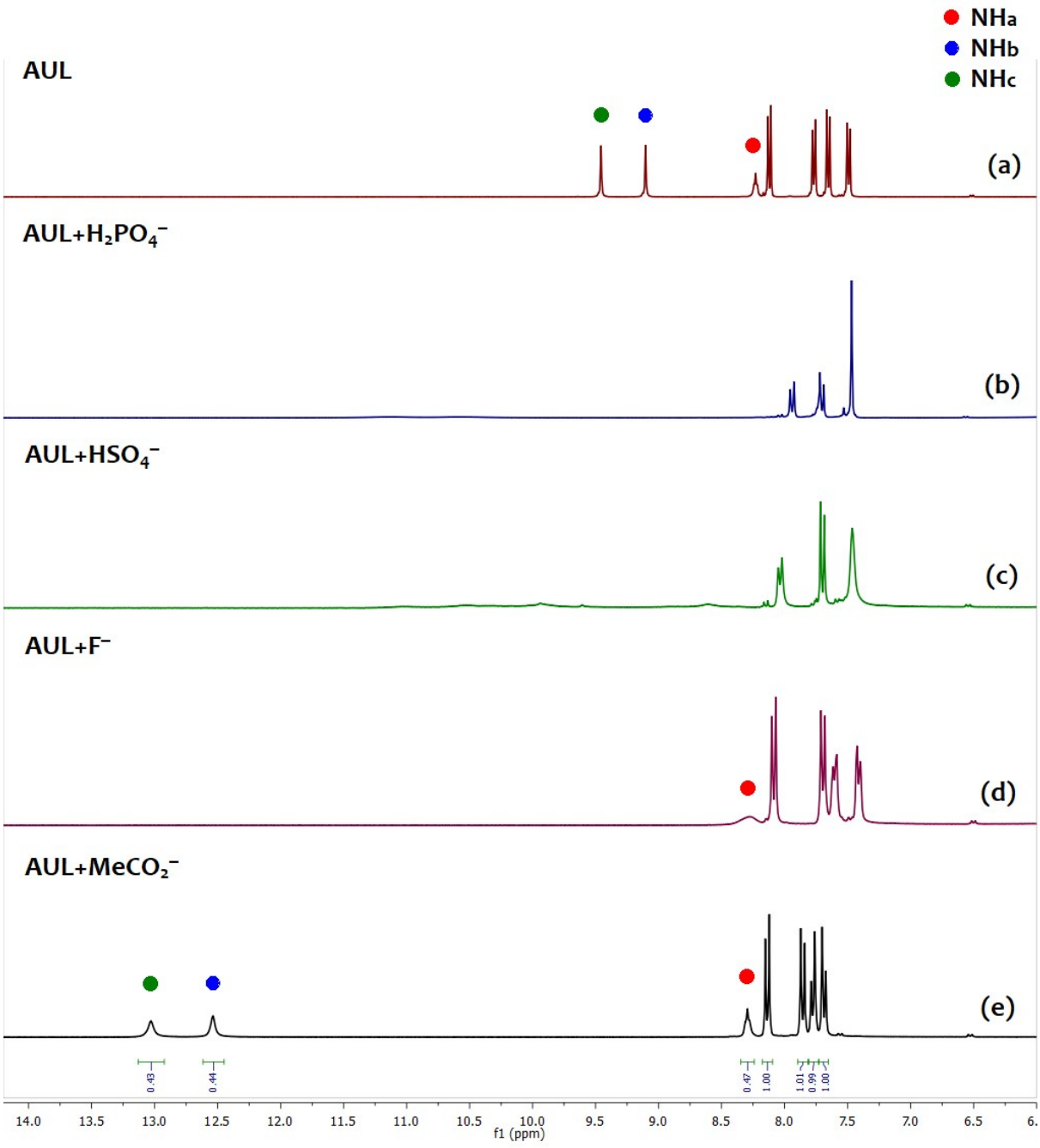

Fig. S10 Aromatic region of ^{1}H-NMR (DMSO-d_6) spectra of **AUL** in the presence of (b) (n-Bu_4N^+)$H_2PO_4^-$, (c) (n-Bu_4N^+)HSO_4^-, (d) (n-Bu_4N^+)F^- and (e) $LiCH_3COO$. (Full spectra are shown below).

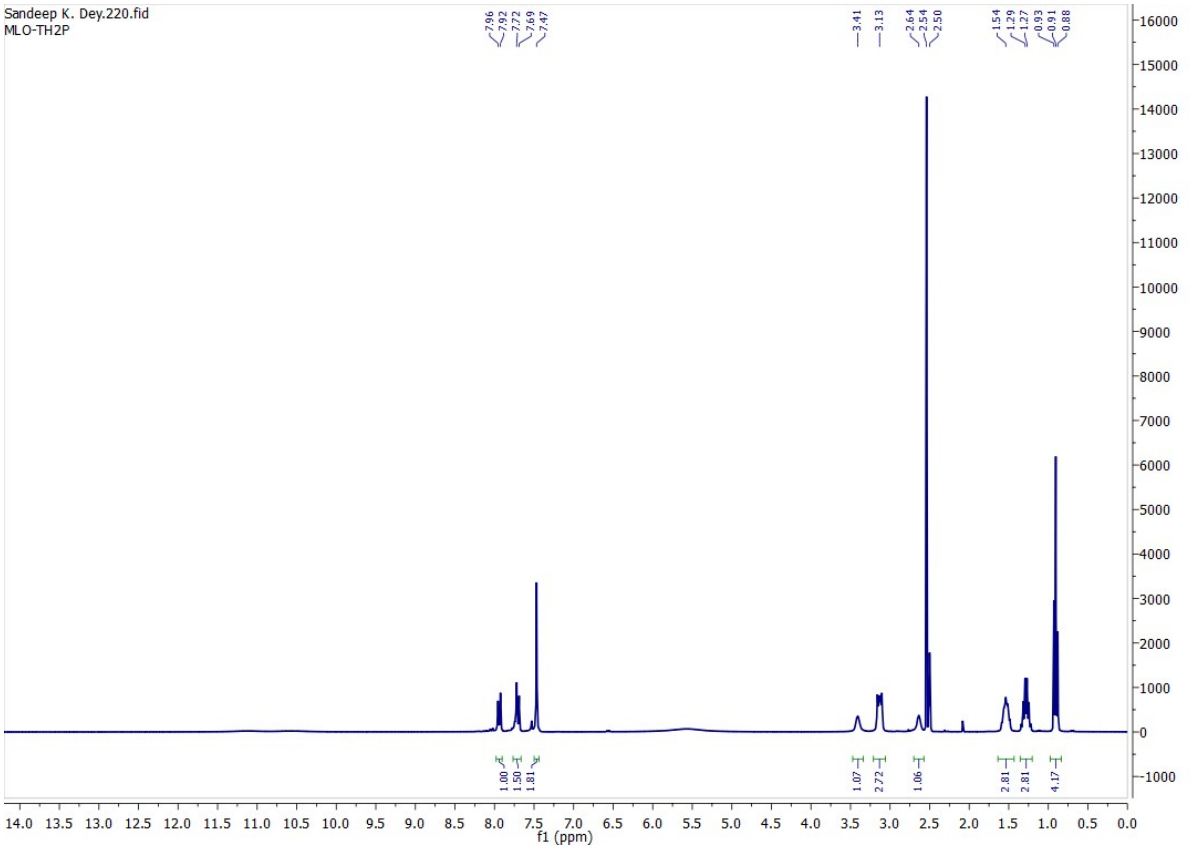

Fig. S11 ^{1}H-NMR spectrum of **AUL** in presence of 2 equivalents of (n-Bu_4N^+)$H_2PO_4^-$ in DMSO-d_6.

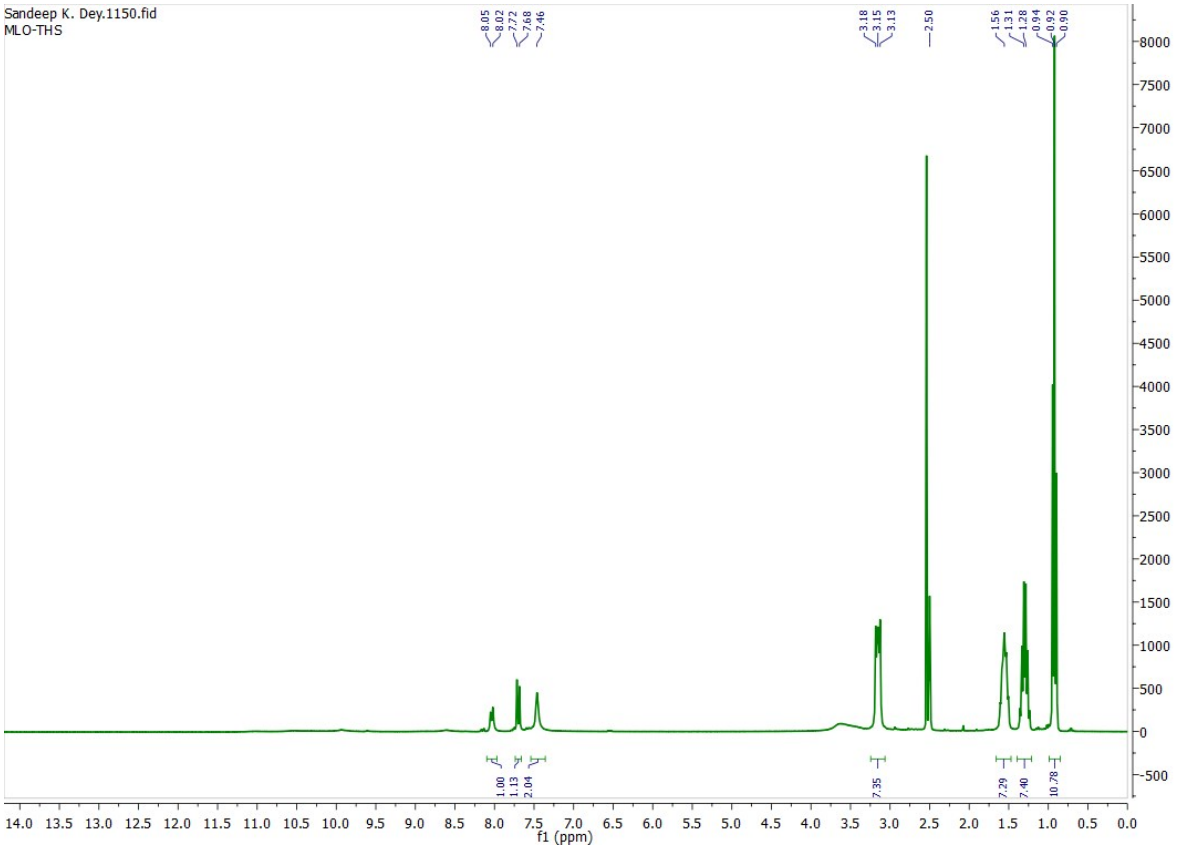

Fig. S12 ^{1}H-NMR spectrum of **AUL** in presence of 4 equivalents of (n-Bu_4N^+)HSO_4^- in DMSO-d_6.

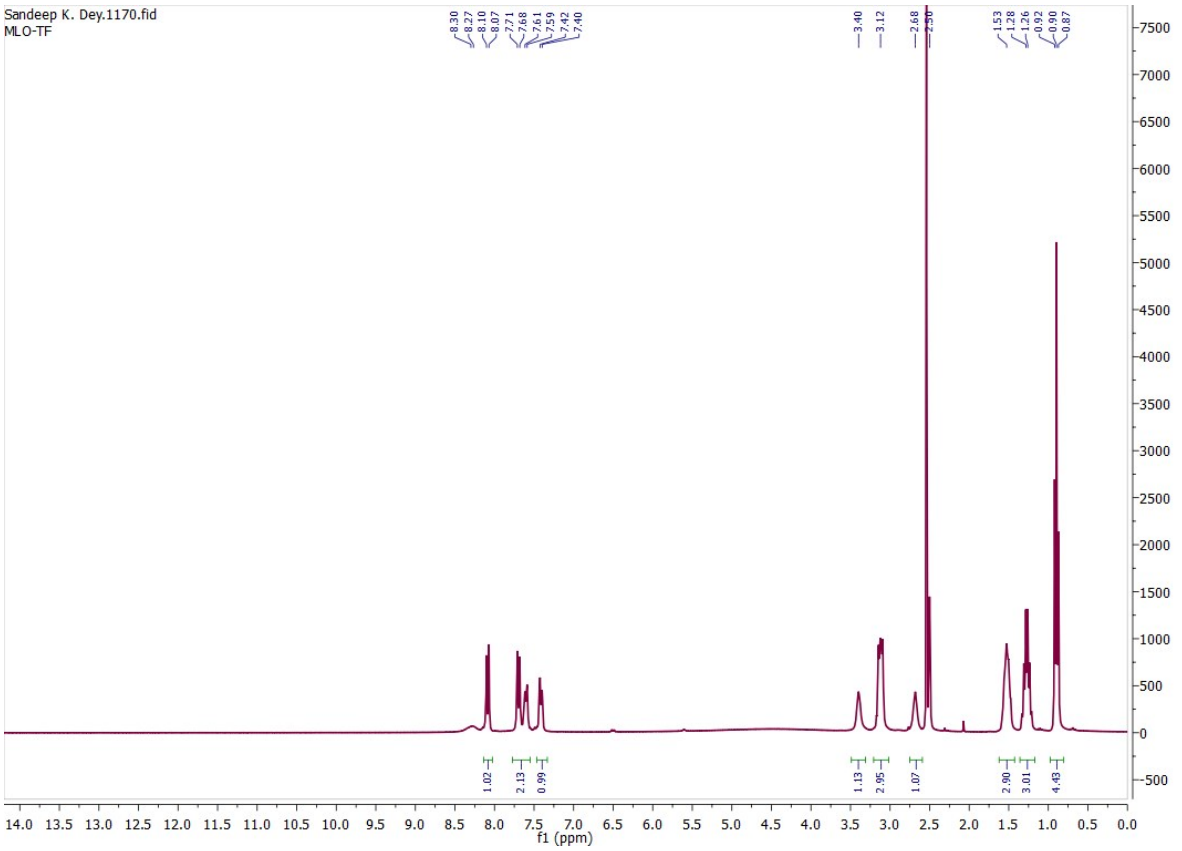

Fig. S13 ^{1}H-NMR spectrum of **AUL** in presence of 2 equivalents of (n-Bu_4N^+)F^- in DMSO-d_6.

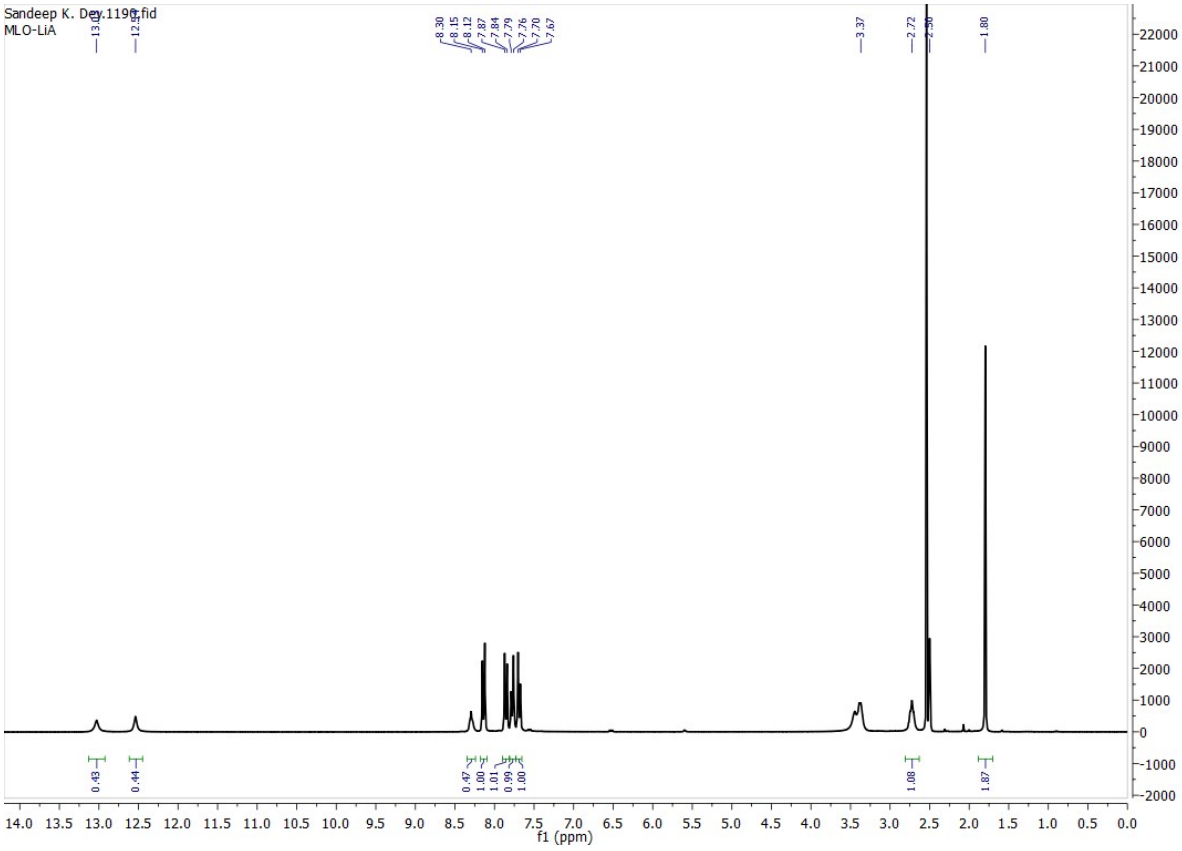

Fig. S14 ^{1}H-NMR spectrum of **AUL** in presence of 4 equivalents of Li acetate in DMSO-d_6.

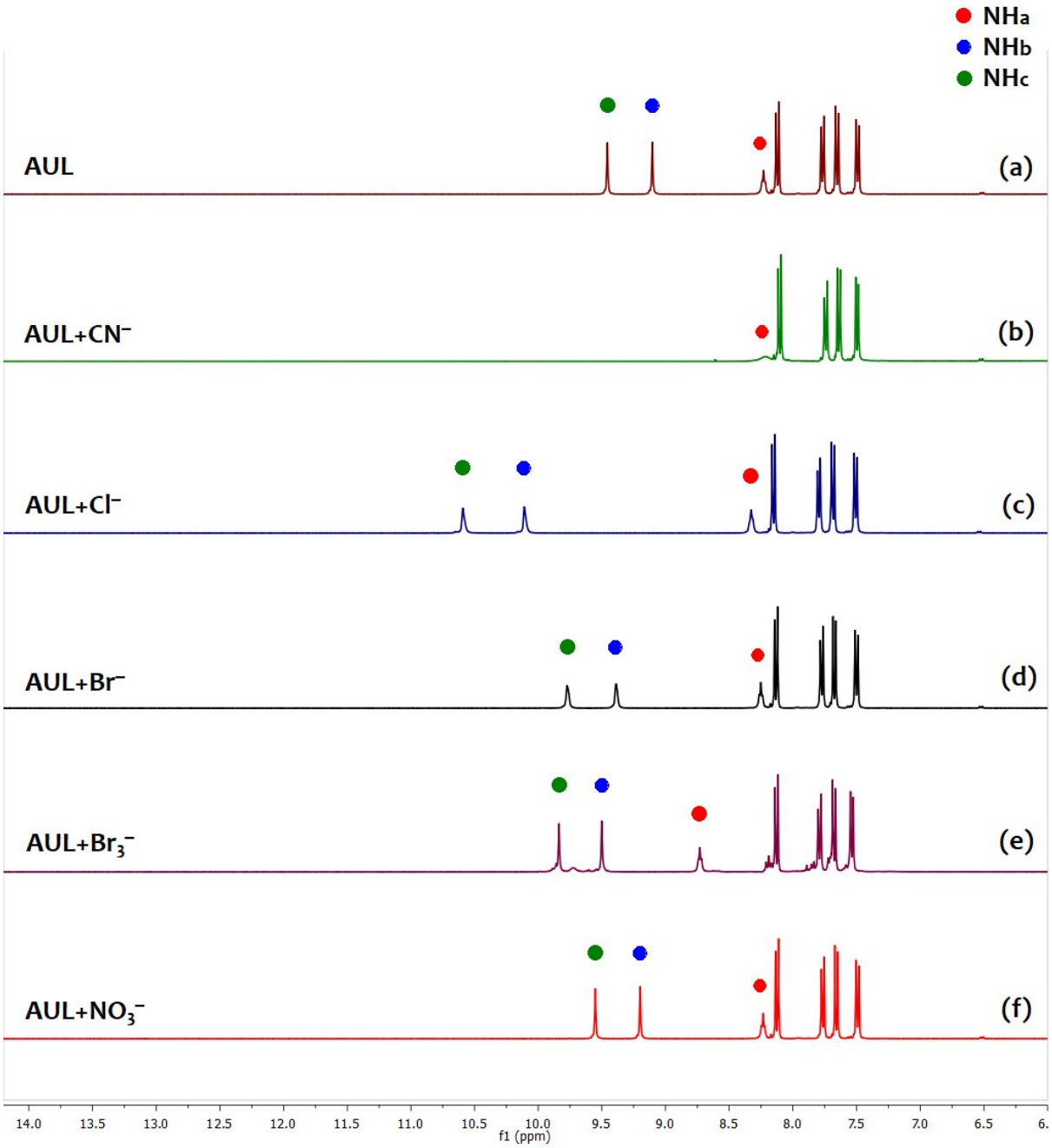

Fig. S15 Aromatic region of ^{1}H-NMR (DMSO-d_6) spectra of **AUL** in the presence of (b) $(Et_4N^+)CN^-$, (c) $(Et_4N^+)Cl^-$, (d) $(n\text{-}Bu_4N^+)Br^-$, (e) $(n\text{-}Bu_4N^+)Br_3^-$ and (f) $(n\text{-}Bu_4N^+)NO_3^-$ (Full spectra are provided below).

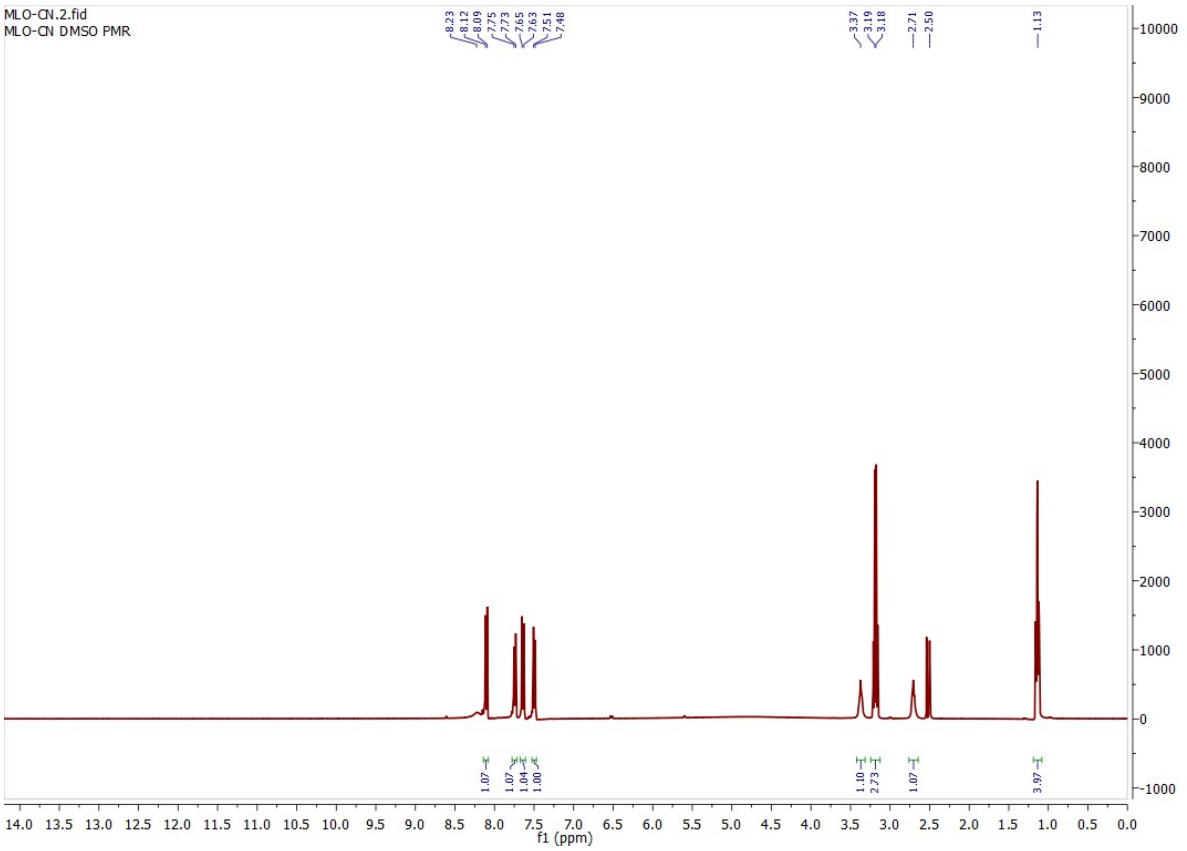

Fig. S16 ^{1}H-NMR spectrum of **AUL** in presence of 2 equivalents of $(Et_4N^+)CN^-$ in DMSO-d_6.

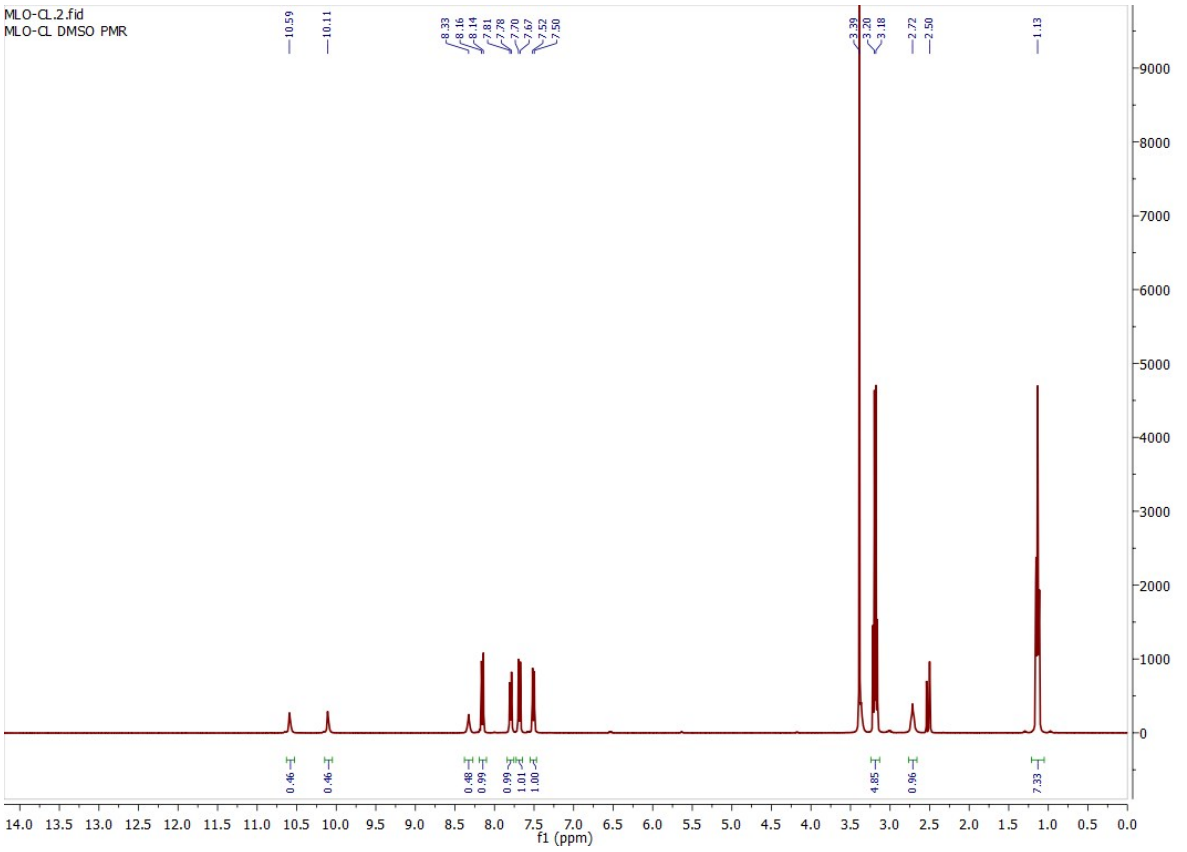

Fig. S17 ^{1}H-NMR spectrum of **AUL** in presence of 3.5 equivalents of $(Et_4N^+)Cl^-$ in DMSO-d_6.

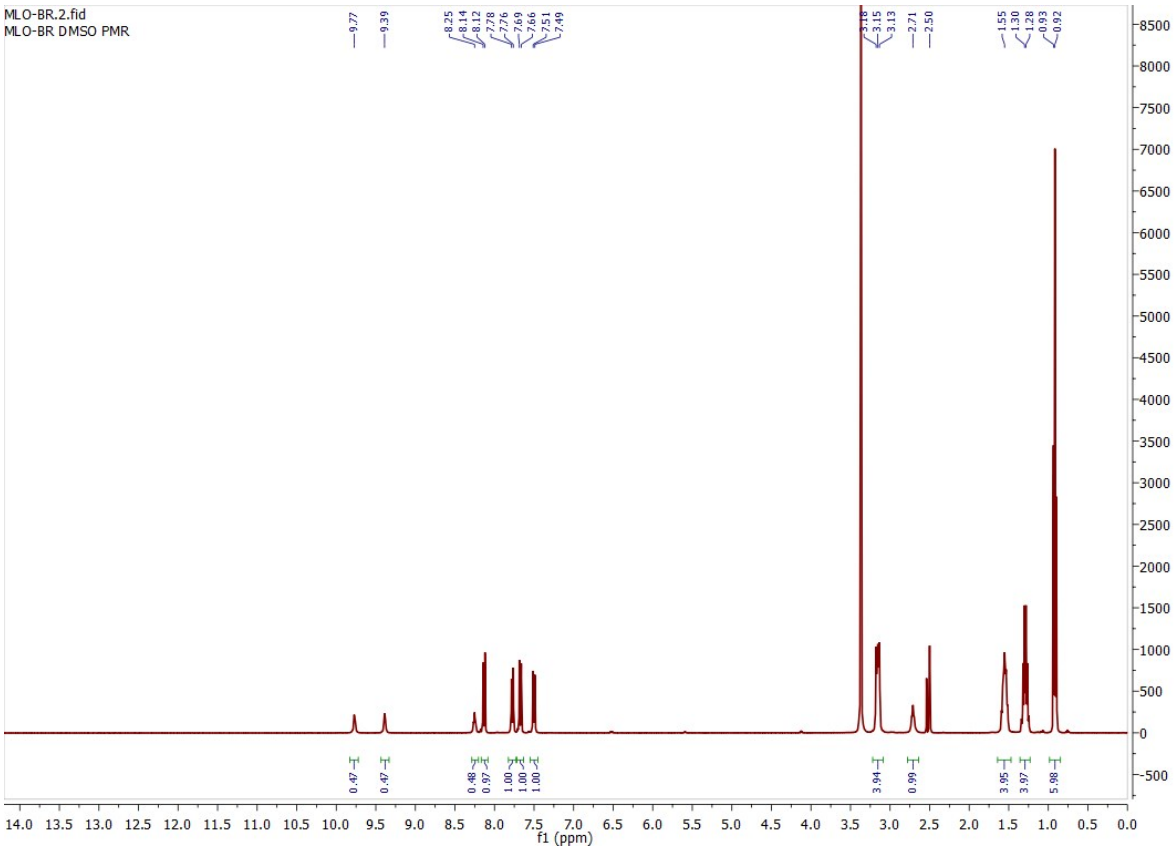

Fig. S18 ^{1}H-NMR spectrum of **AUL** in presence of 3 equivalents of (n-Bu_4N^+)Br^- in DMSO-d_6.

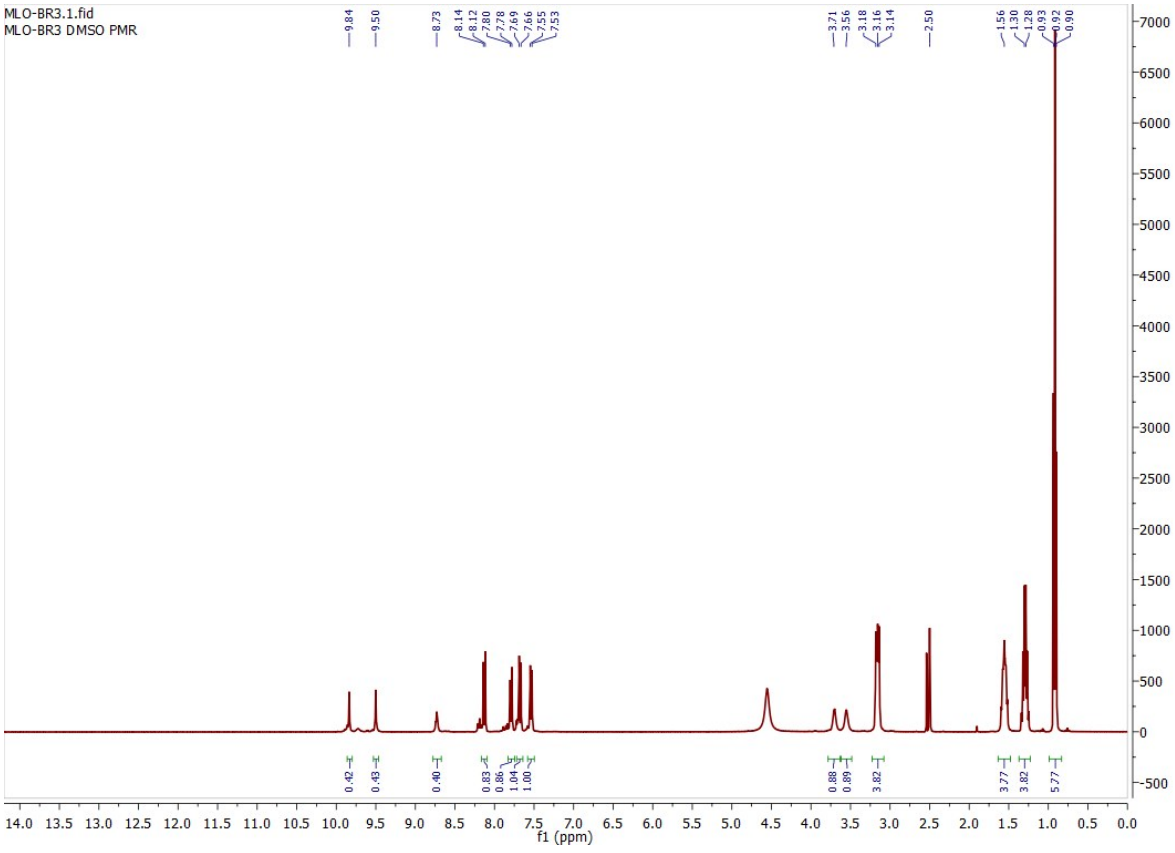

Fig. S19 ^{1}H-NMR spectrum of **AUL** in presence of 3 equivalents of (n-Bu_4N^+)Br_3^- in DMSO-d_6.

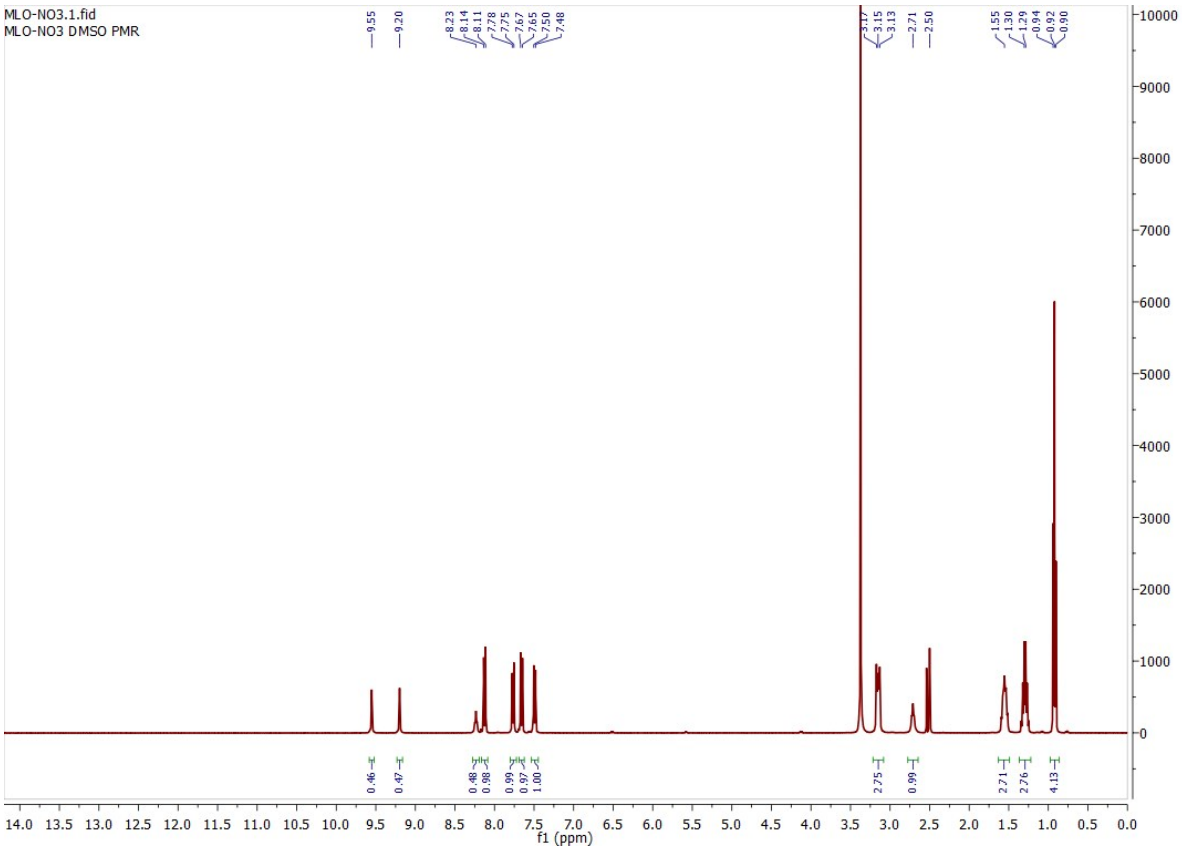

Fig. S20 ^{1}H-NMR spectrum of **AUL** in presence of 2 equivalents of $(n\text{-}Bu_4N^+)NO_3^-$ in DMSO-d_6.

4. Characterization of hydrogenphosphate complex [(n-$Bu_4N)_2$(AUL·HPO_4)·DMSO·CH_3CN].

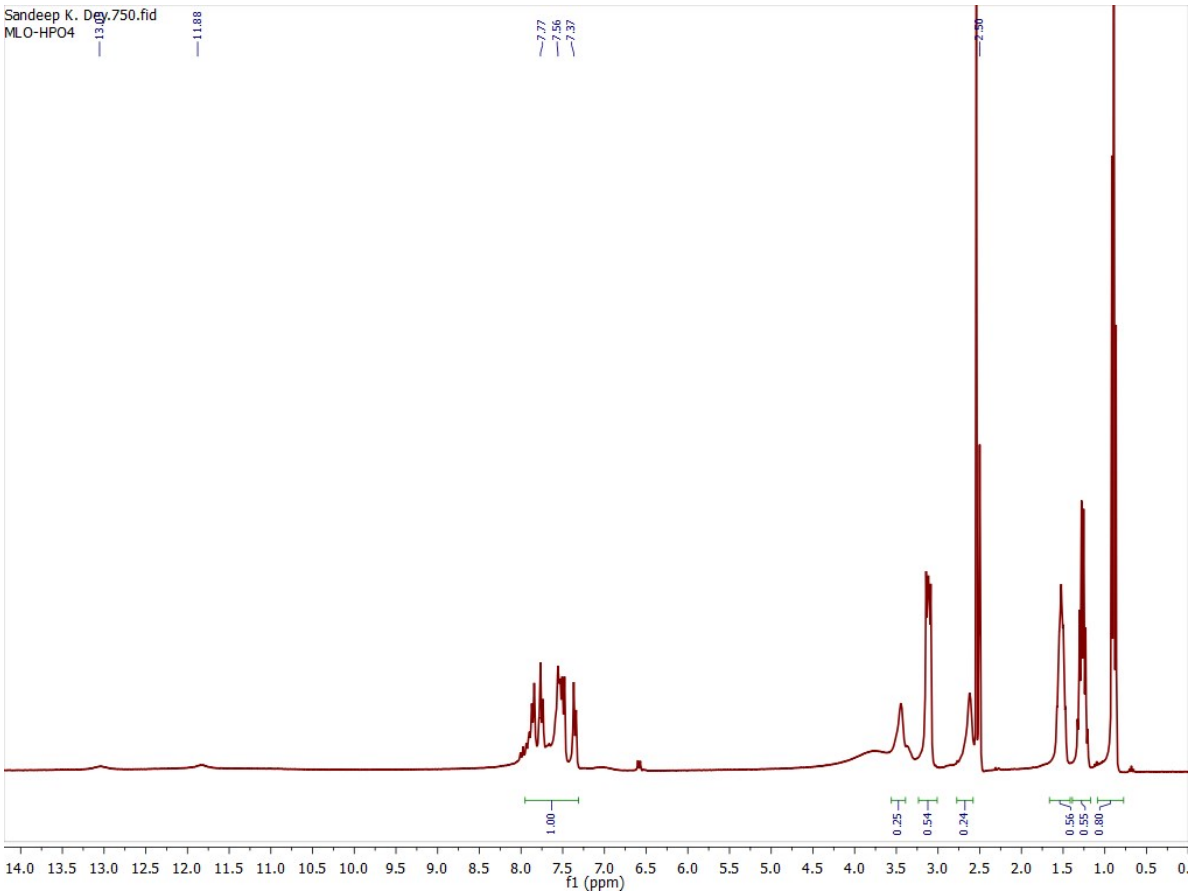

Fig. S21 ^{1}H-NMR spectrum of [(n-$Bu_4N)_2$(**AUL**·HPO_4)·DMSO·CH_3CN] in DMSO-d_6.

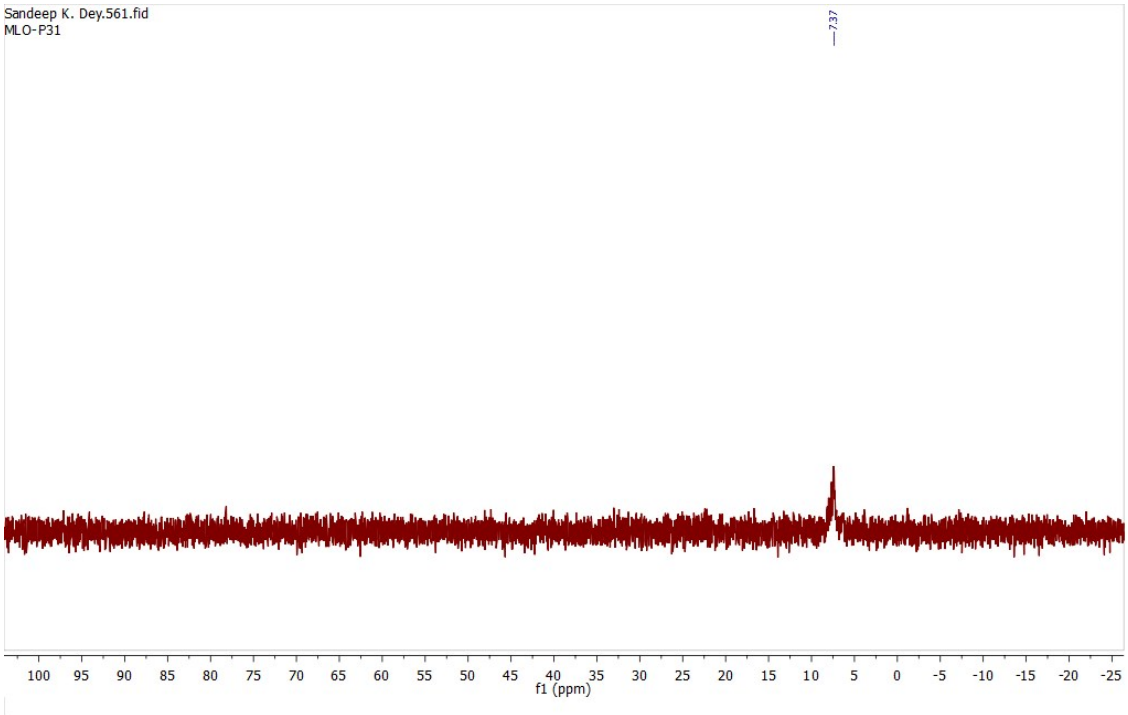

Fig. S22 ^{31}P-NMR spectrum of [(n-$Bu_4N)_2$(**AUL**·HPO_4)·DMSO·CH_3CN] in DMSO-d_6.

5. DFT optimized structures of receptor-anion complexes and binding energy calculations.

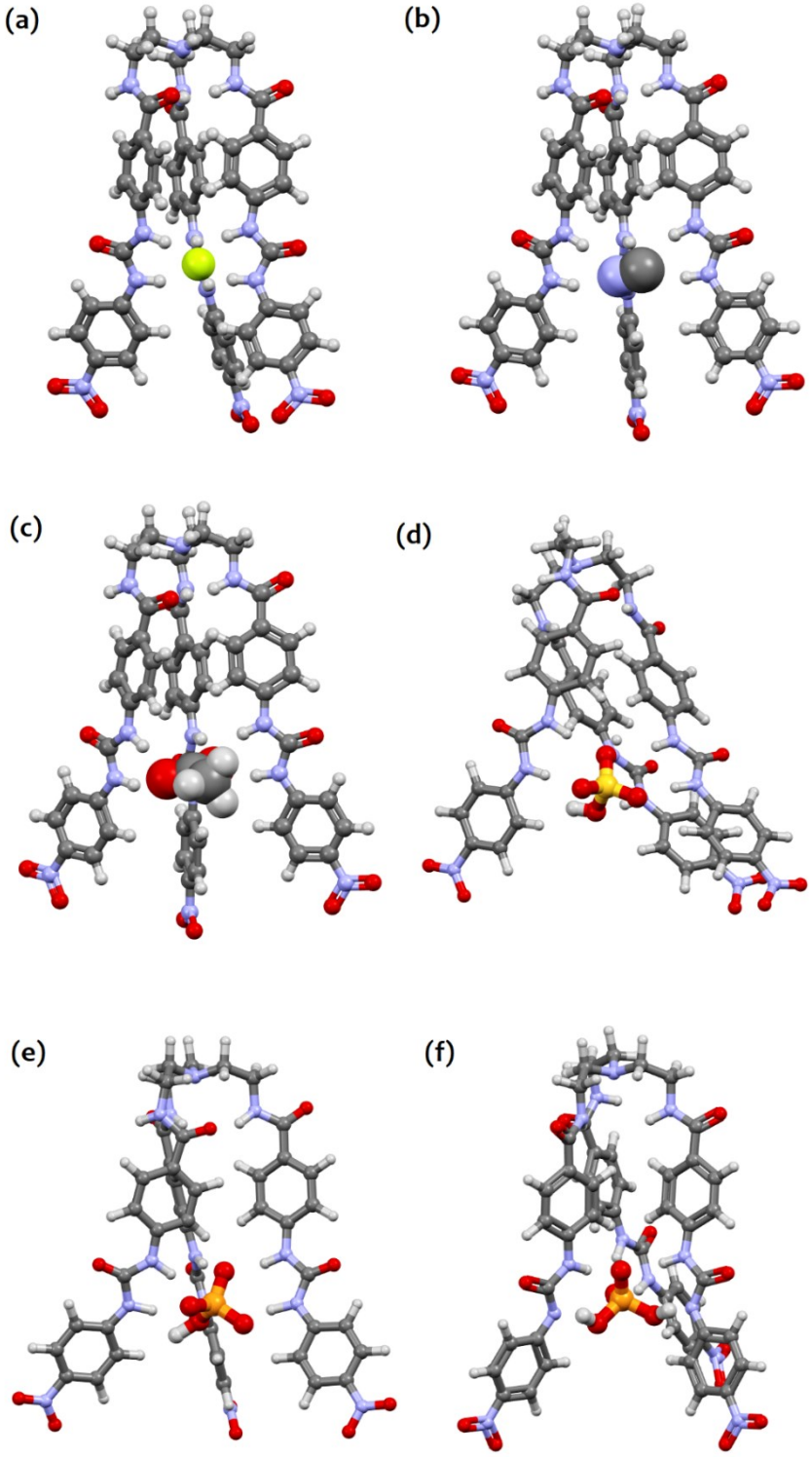

Fig. S23 DFT energy optimized structures of receptor-anion complexes between urea-based receptor **AUL** and anions of different geometry such as fluoride, cyanide, acetate, hydrogensulfate and hydrogenphosphate, (a) (**AUL**·F)$^{-}$, (b) (**AUL**·CN)$^{-}$ (c) (**AUL**·CH_3COO)$^{-}$ (d) (**AUL**·HSO_4)$^{-}$, (e) (**AUL**·HPO_4)$^{2-}$. (f) (**AUL**·PO_4)$^{3-}$.

Table S1: Binding energy (B.E.) of receptor-anion hydrogen bonded complexes of **AUL** with different anions based on DFT calculations, B.E. = $(E_{receptor} + E_{anion}) - E_{complex}$.

	E (complex)	**E** (receptor)	**E** (anion)	**B.E.** (Hartree)	**B.E.** (kJ/mol)
(**AUL**·HPO_4)$^{2-}$	-4111.31015	-3468.28034	-642.624919	0.40	1063.04
(**AUL**·CN)$^-$	-3563.60132	-3470.63918	-92.756873	0.21	538.912
(**AUL**·CH_3COO)$^-$	-3699.28655	-3470.63918	-228.357429	0.29	761.231
(**AUL**·F)$^-$	-3570.63658	-3470.63918	-99.7047869	0.29	768.249
(**AUL**·HSO_4)$^-$	-4167.98610	-3468.28034	-699.521466	0.18	483.874
(**AUL**·SO_4)$^{2-}$	-4169.89803	-3470.57966	-698.930327	0.39	1018.81
(**AUL**·PO_4)$^{3-}$	-4113.10941	-3470.63918	-641.60904	0.86	2261.06

6. Characterization of hydrogenphosphate complex obtained from liquid-liquid (DCM/water) extraction of phosphate (K_3PO_4) by AUL in presence of n-Bu_4N^+ salts of F^-/OH^-/CH_3COO^-.

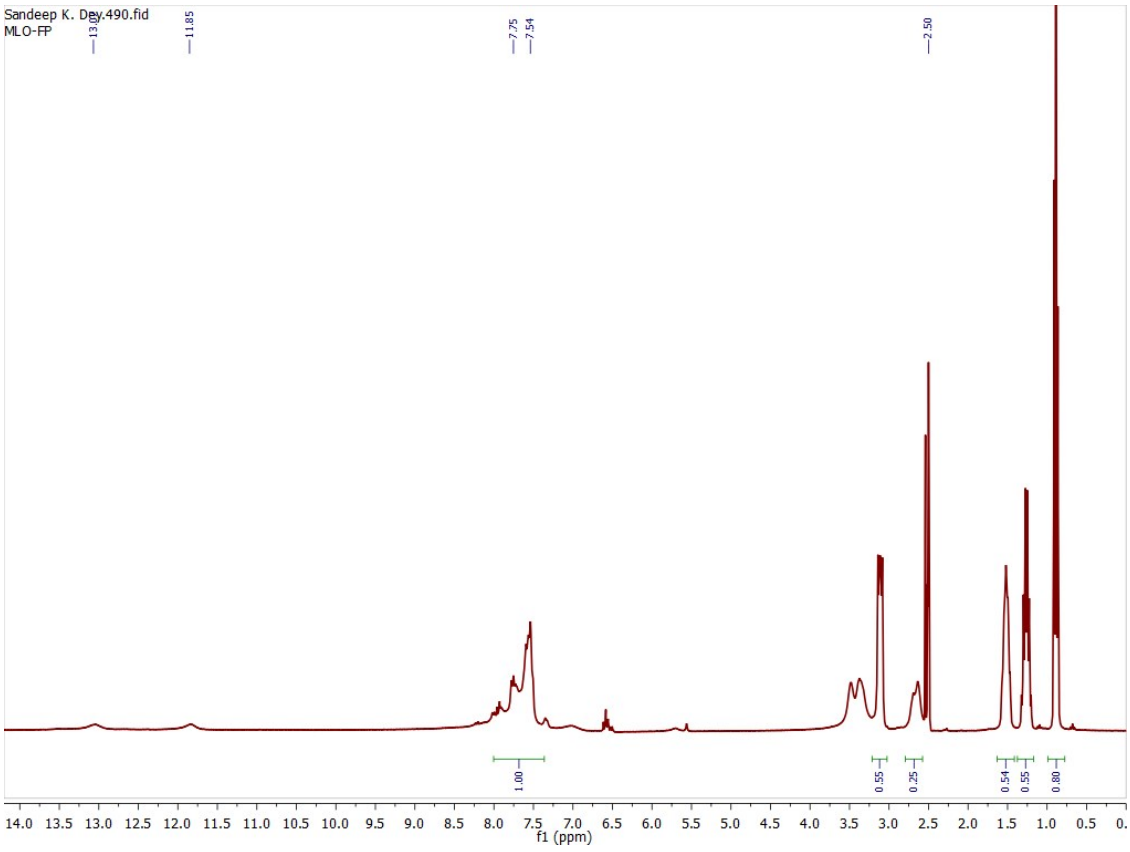

Fig. S24 ^{1}H-NMR spectrum of [(n-Bu_4N)$_2$(**AUL**·HPO_4)] (DMSO-d_6) obtained from liquid-liquid (DCM/water) extraction of phosphate by **AUL** in the presence of 2 equiv. (n-Bu_4N^+)F^-.

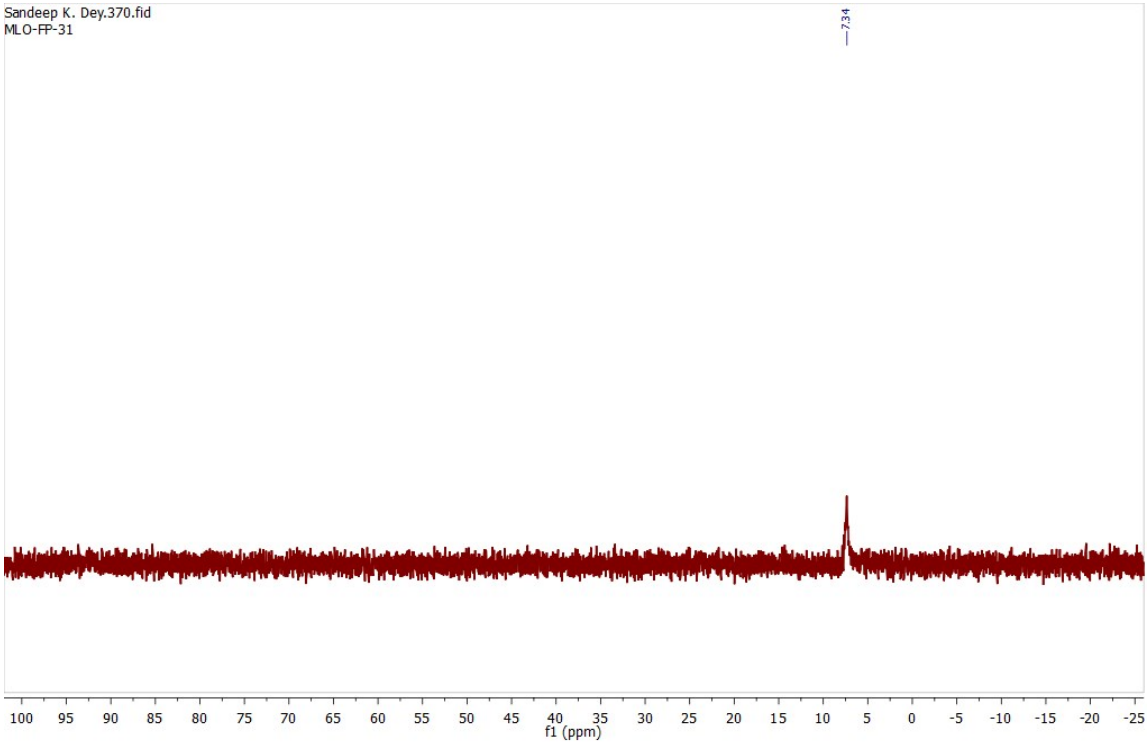

Fig. S25 ^{31}P-NMR spectrum of [(n-$Bu_4N)_2$(**AUL**·HPO_4)] (DMSO-d_6) obtained from liquid-liquid (DCM/water) extraction of phosphate by **AUL** in the presence of 2 equiv. (n-Bu_4N^+)F^-.

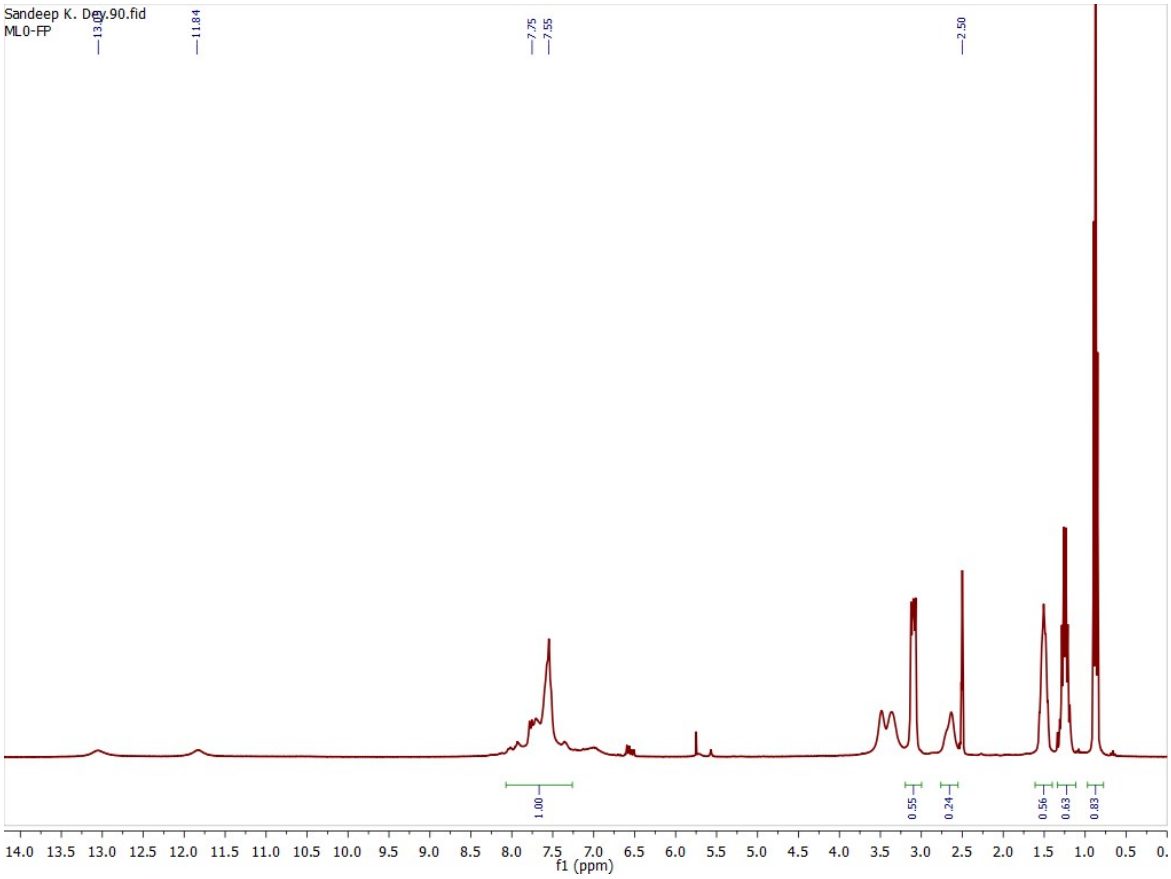

Fig. S26 ^{1}H-NMR spectrum of [(n-$Bu_4N)_2$(**AUL**·HPO_4)] (DMSO-d_6) obtained from liquid-liquid (DCM/water) extraction of phosphate by **AUL** in the presence of 2 equiv. (n-Bu_4N^+)CH_3COO^-.

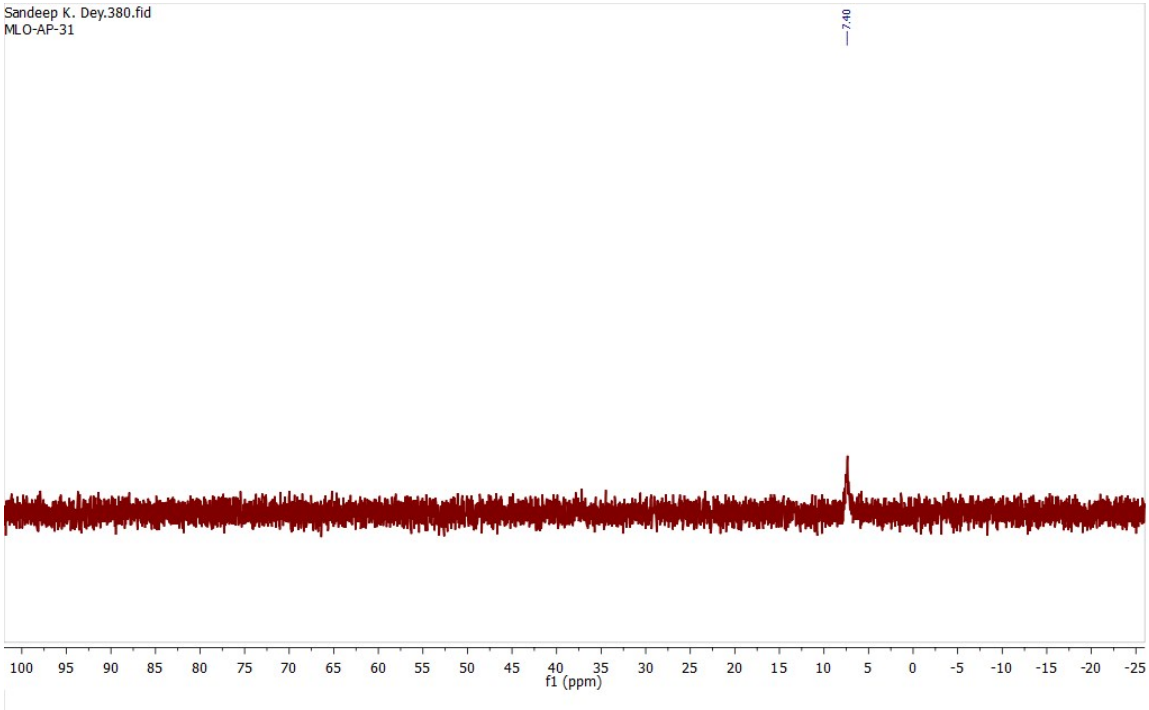

Fig. S27 ^{31}P-NMR spectrum of [(n-Bu_4N)$_2$(**AUL**·HPO_4)] (DMSO-d_6) obtained from liquid-liquid (DCM/water) extraction of phosphate by **AUL** in the presence of 2 equiv. (n-Bu_4N^+)CH_3COO^-.

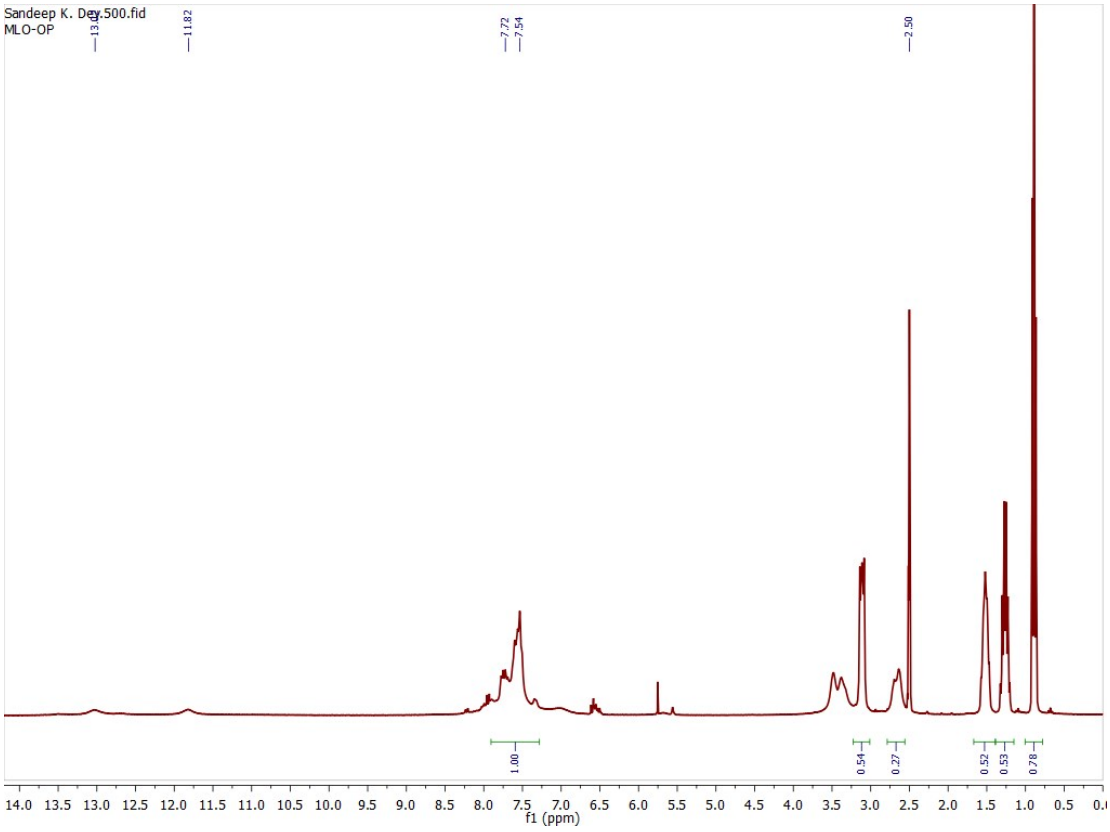

Fig. S28 ^{1}H-NMR spectrum of [(n-Bu_4N)$_2$(**AUL**·HPO_4)] (DMSO-d_6) obtained from liquid-liquid extraction of phosphate by **AUL** in the presence of 2 equiv. (n-Bu_4N^+)OH^-.

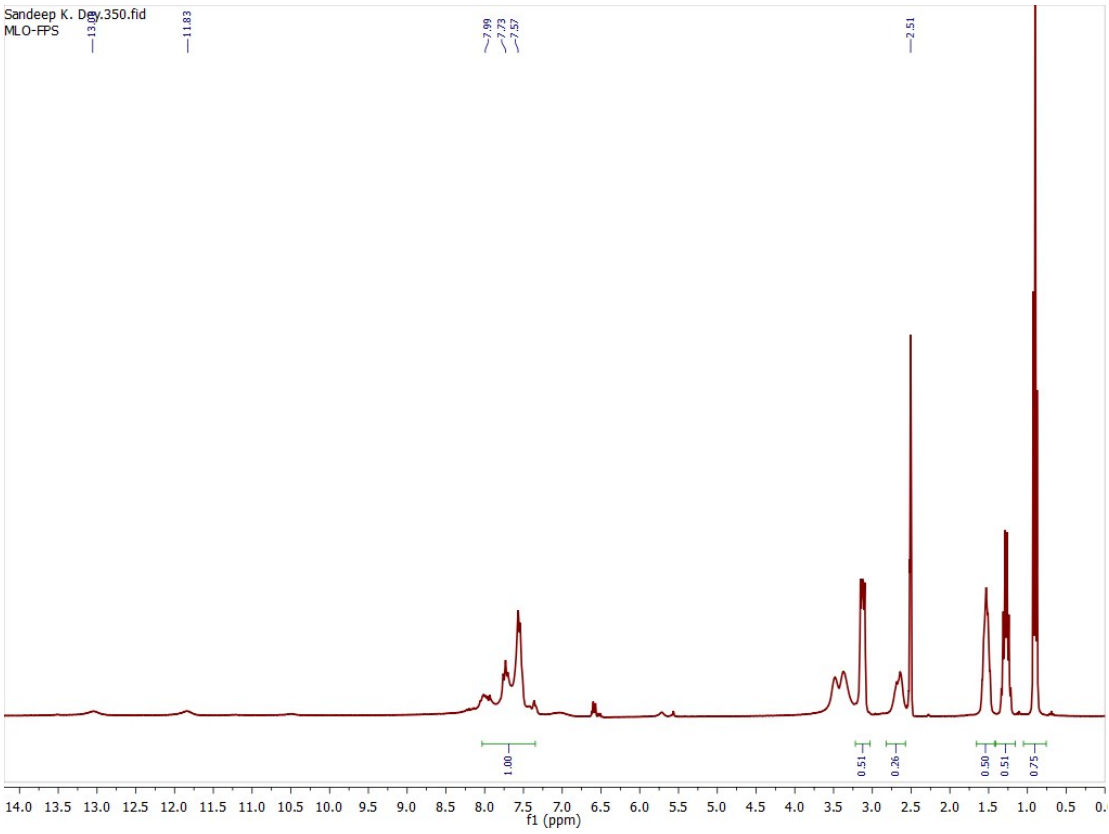

Fig. S29 ^{1}H-NMR spectrum of [(n-Bu_4N)$_2$(**AUL**·HPO_4)] (DMSO-d_6) obtained from liquid-liquid (DCM/water) extraction of phosphate by **AUL** in the presence of (n-Bu_4N^+)F^- and Na_2SO_4.

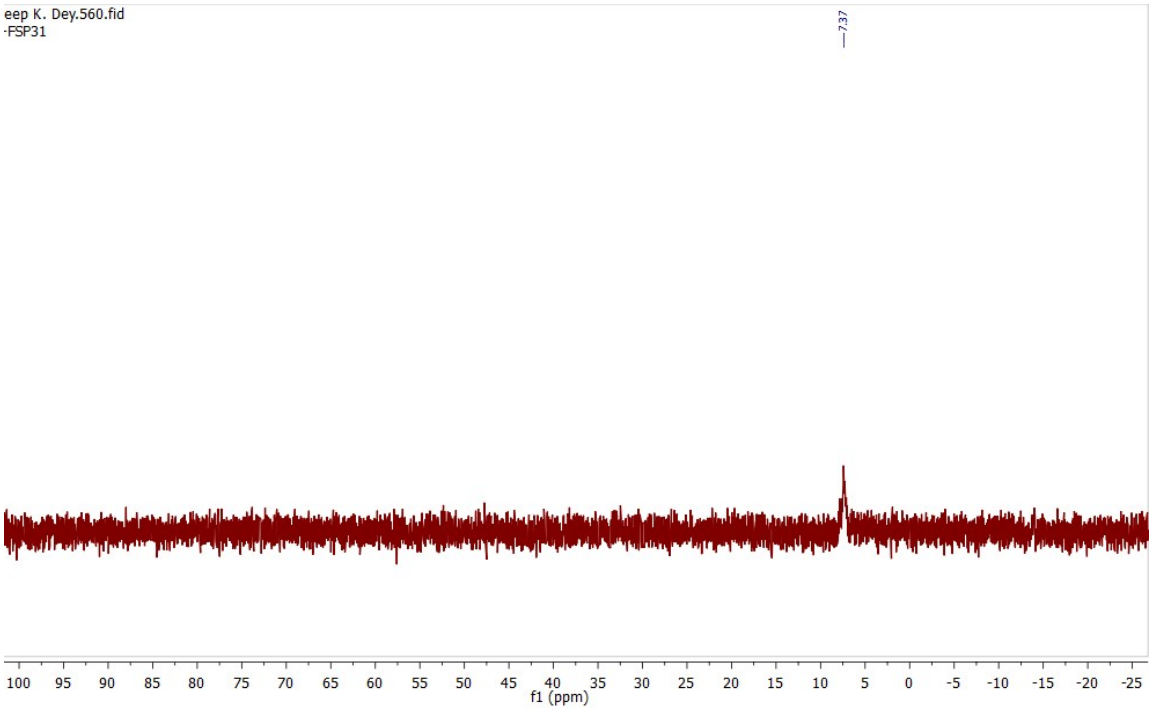

Fig. S30 ^{31}P-NMR spectrum of [(n-Bu_4N)$_2$(**AUL**·HPO_4)] (DMSO-d_6) obtained from liquid-liquid (DCM/water) extraction of phosphate by AUL in the presence of (n-Bu_4N^+)F^- and Na_2SO_4.

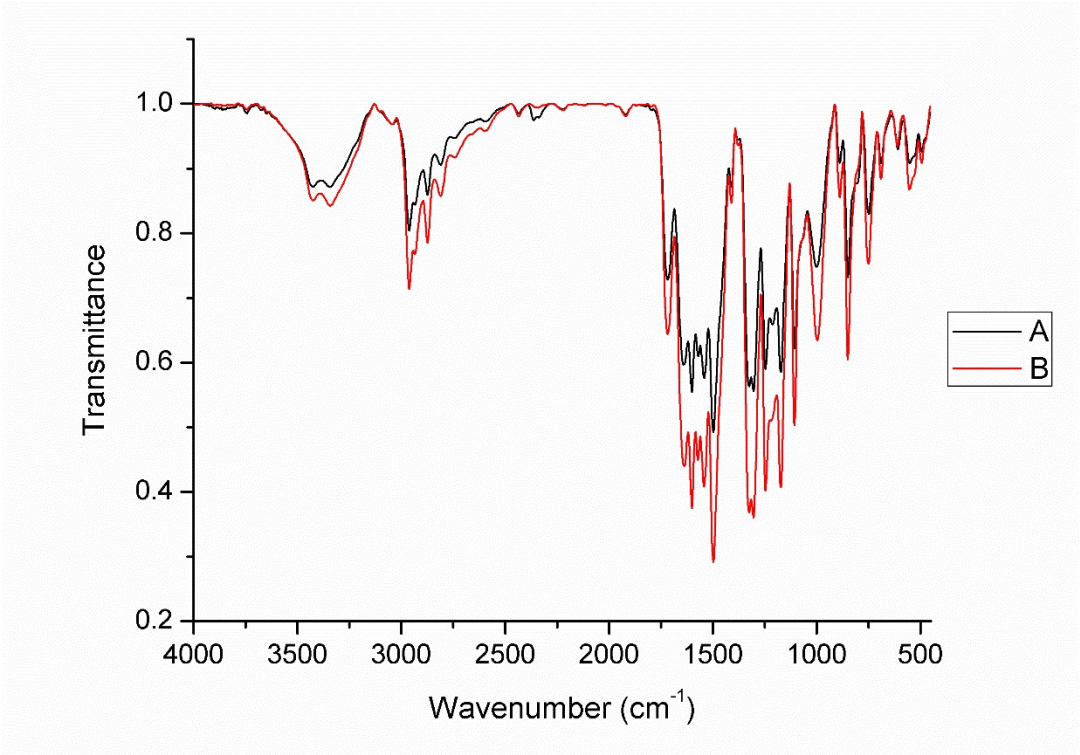

Fig. S31 FT-IR spectra of [(n-$Bu_4N)_2$(**AUL**·HPO_4)] obtained from liquid-liquid extraction of phosphate from water by **AUL** in the presence of (A) (n-Bu_4N^+)F^- (B) (n-Bu_4N^+)F^- and Na_2SO_4.

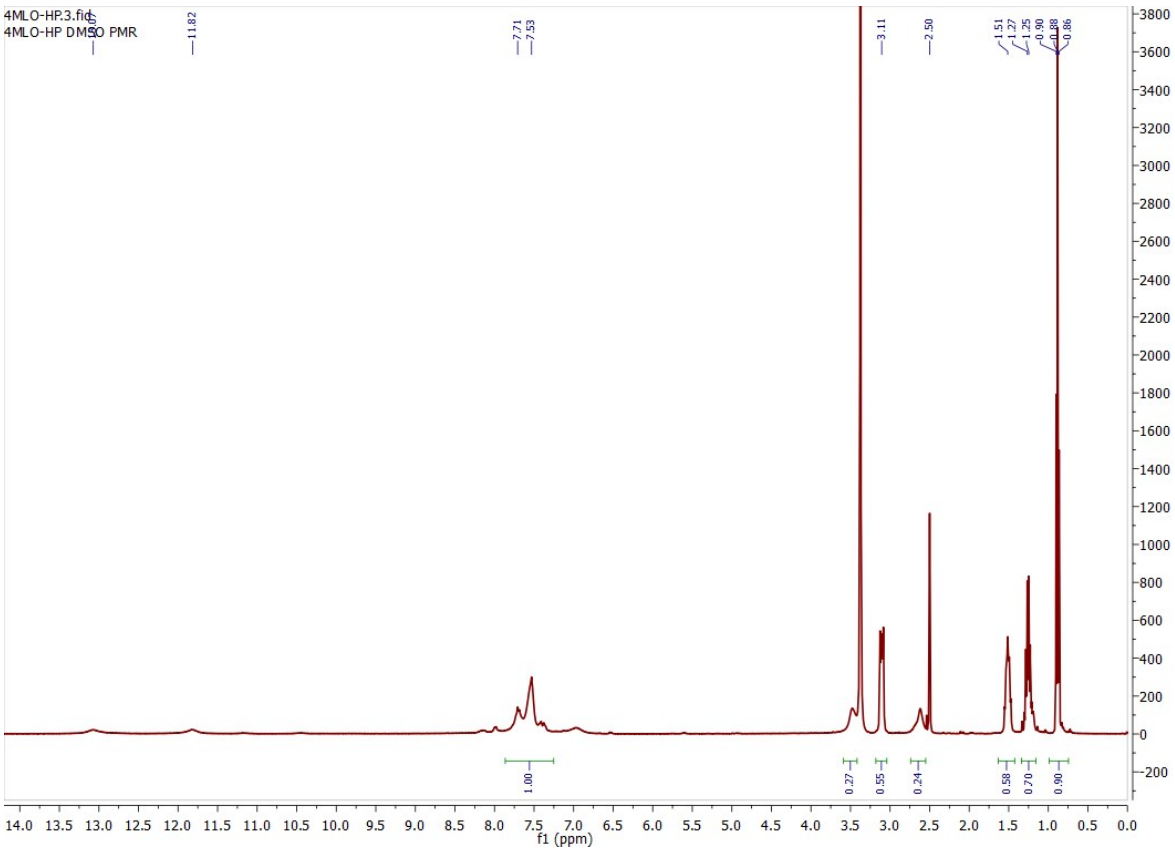

Fig. S32 ^{1}H-NMR spectrum of [(n-$Bu_4N)_2$(**AUL**·HPO_4)] (DMSO-d_6) obtained from liquid-liquid (DCM/water) extraction of phosphate by **AUL** in the presence of (n-Bu_4N^+)$H_2PO_4^-$.

7. ^{1}H-NMR spectra of AAL in the presence of quaternary ammonium (n-Bu_4N^+/ Et_4N^+) salts.

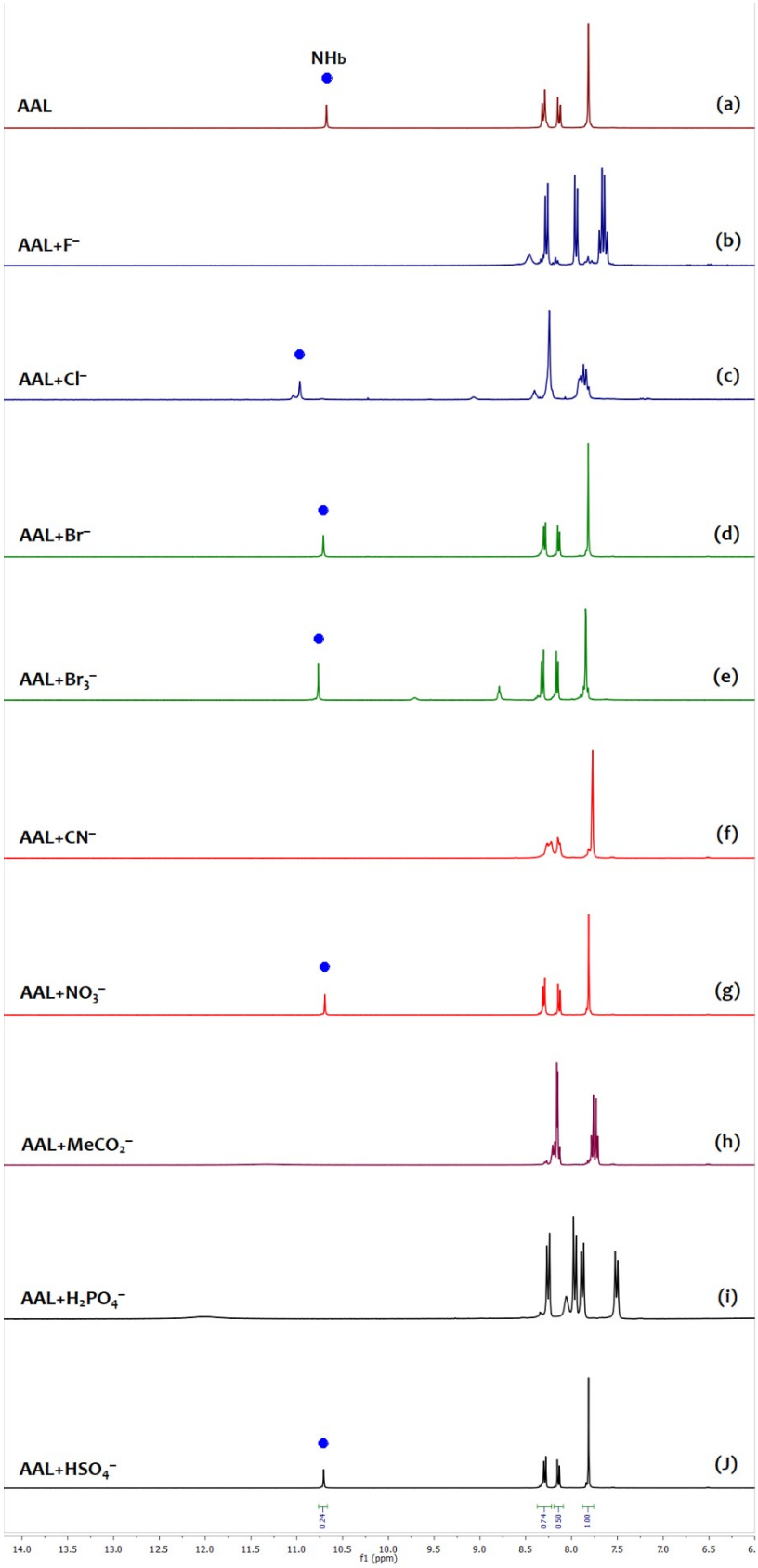

Fig. S33 Aromatic region of ^{1}H-NMR (DMSO-d_6) spectra of **AAL** in the presence of quaternary ammonium salts of different anions (Full spectra are provided below).

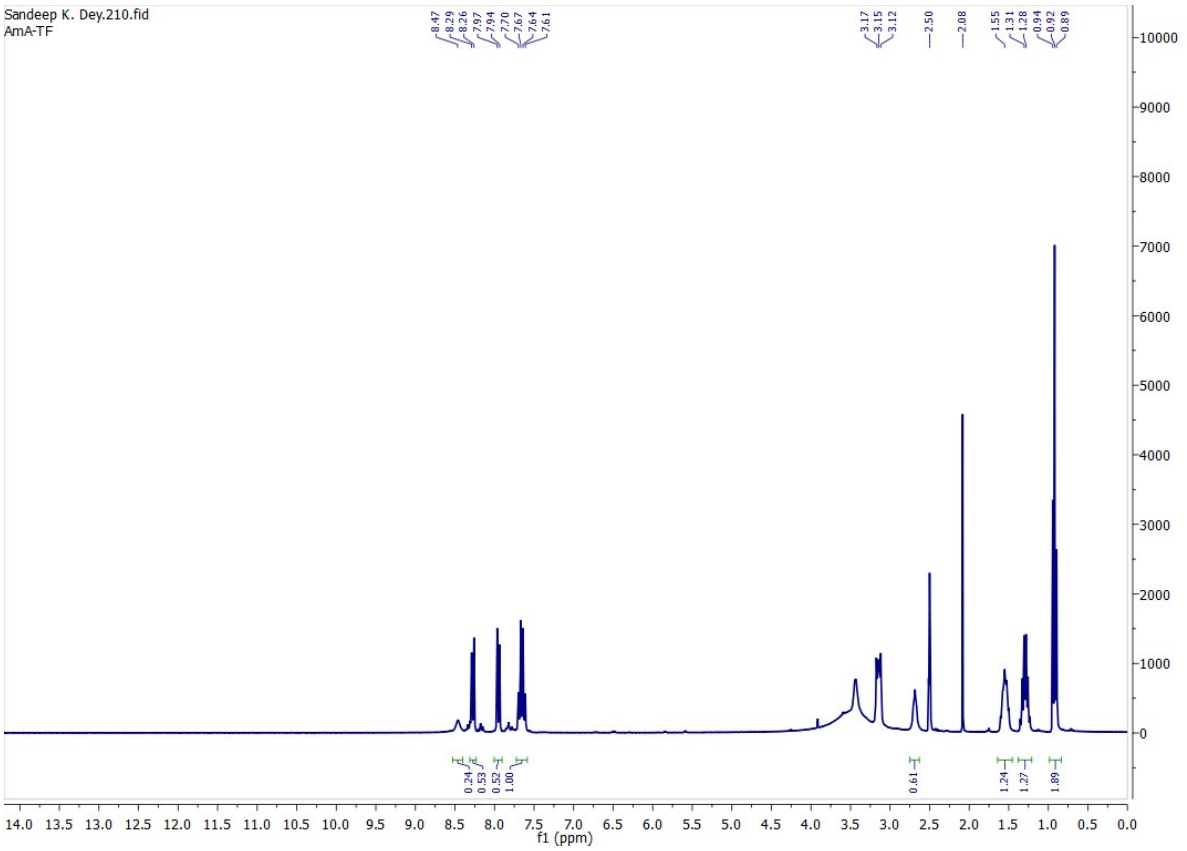

Fig. S34 ^{1}H-NMR spectrum of **AAL** in presence of 2 equivalents of (n-Bu_4N^+)F^- in DMSO-d_6.

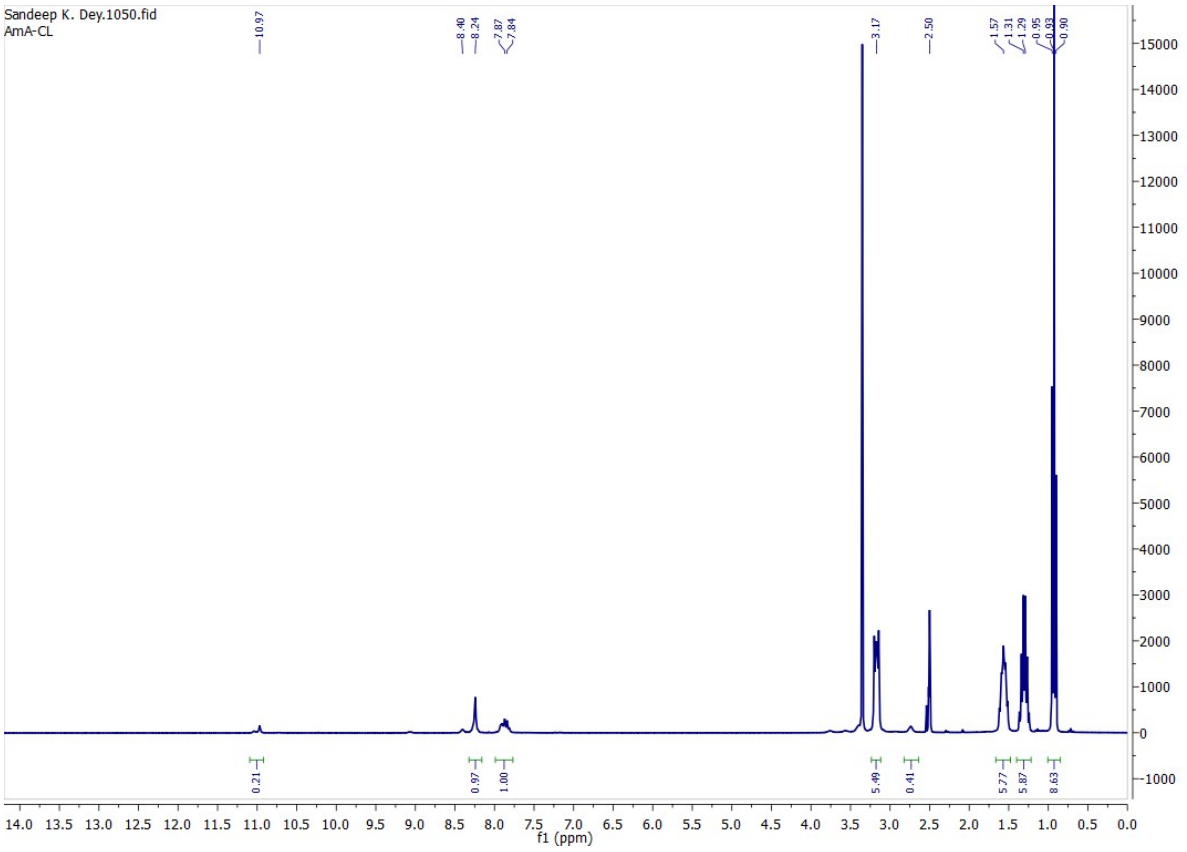

Fig. S35 ^{1}H-NMR spectrum of **AAL** in presence of 4 equivalents of (n-Bu_4N^+)Cl^- in DMSO-d_6.

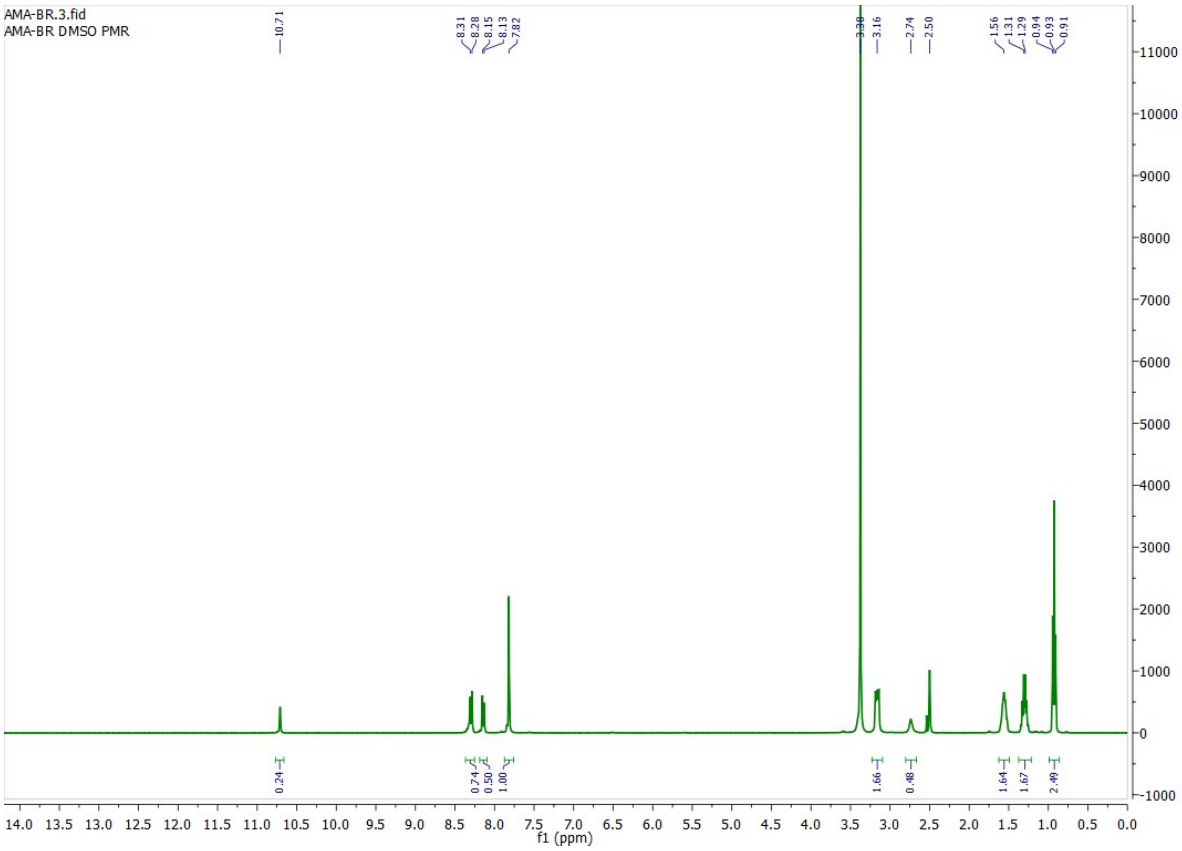

Fig. S36 ^{1}H-NMR spectrum of **AAL** in presence of 2.5 equivalents of (n-Bu_4N^+)Br^- in DMSO-d_6.

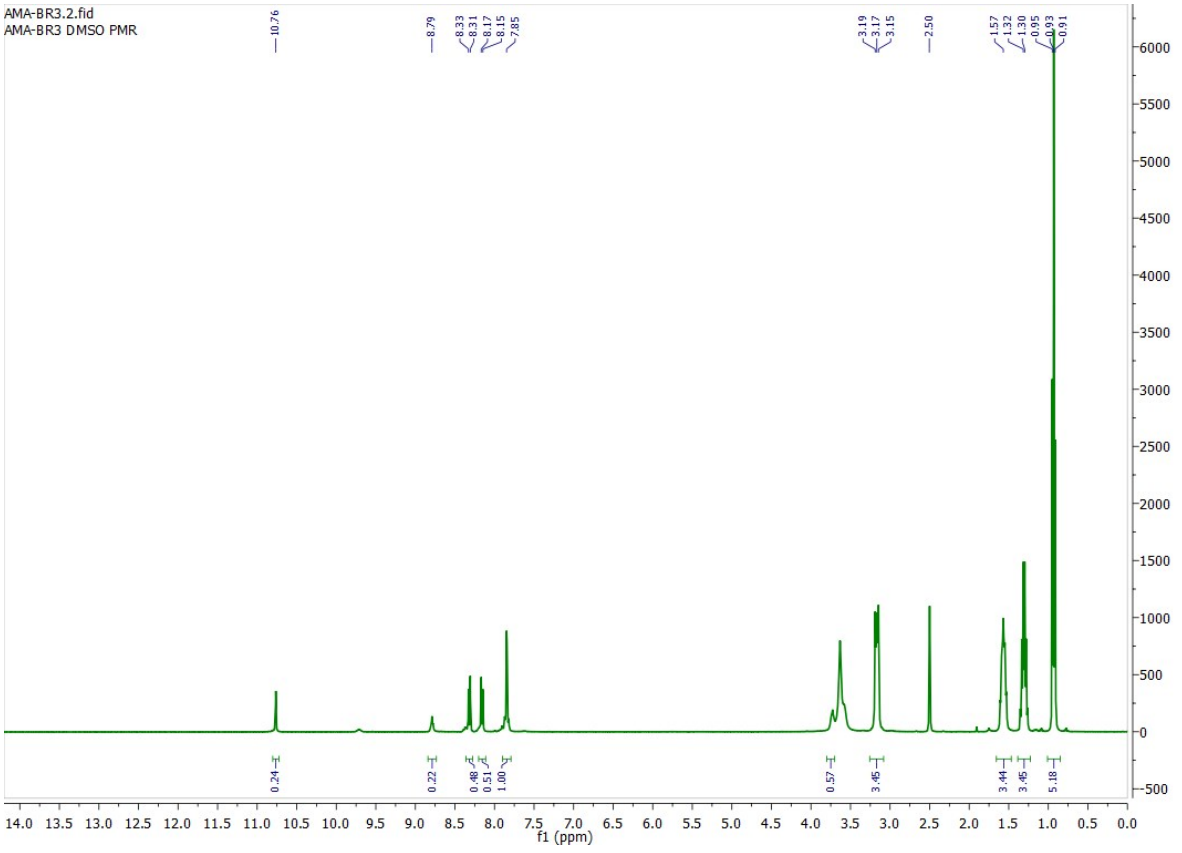

Fig. S37 ^{1}H-NMR spectrum of **AAL** in presence of 4 equivalents of (n-Bu_4N^+)Br_3^- in DMSO-d_6.

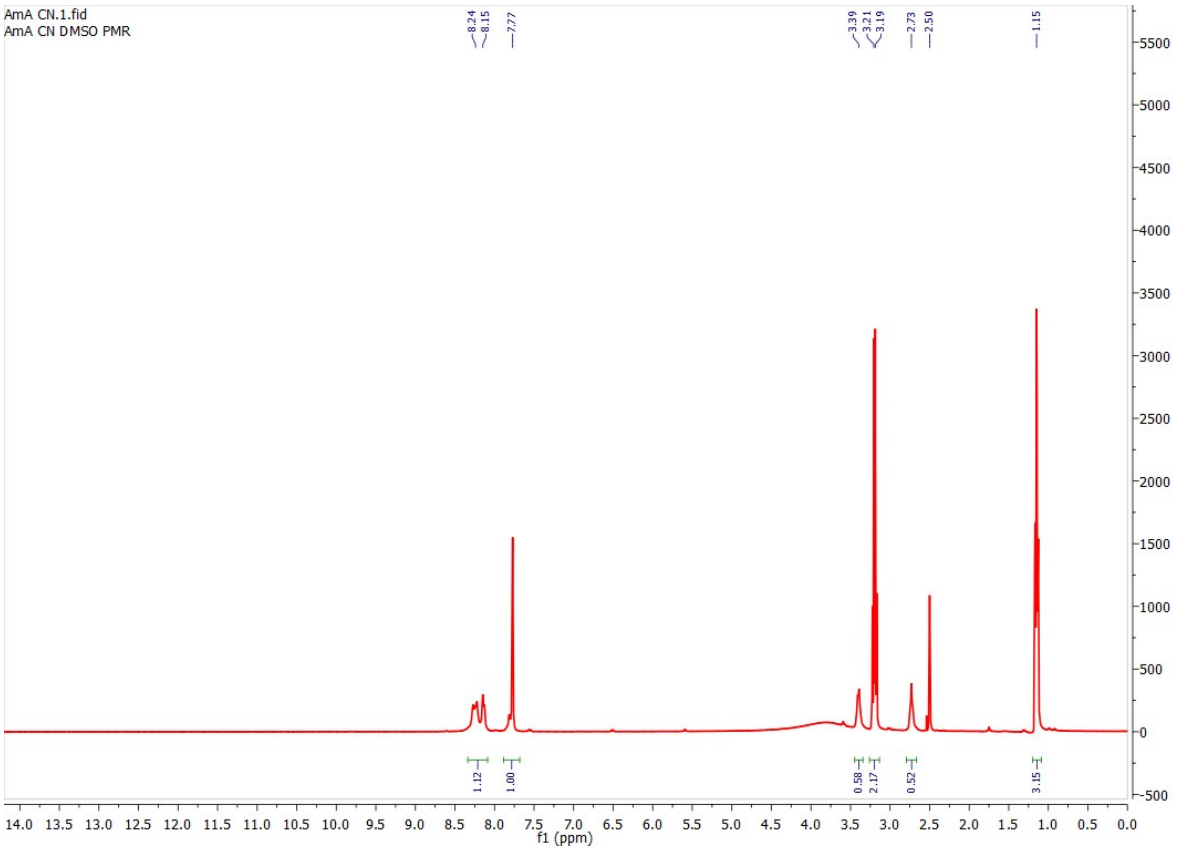

Fig. S38 ^{1}H-NMR spectrum of **AAL** in presence of 4 equivalents of $(Et_4N^+)CN^-$ in DMSO-d_6.

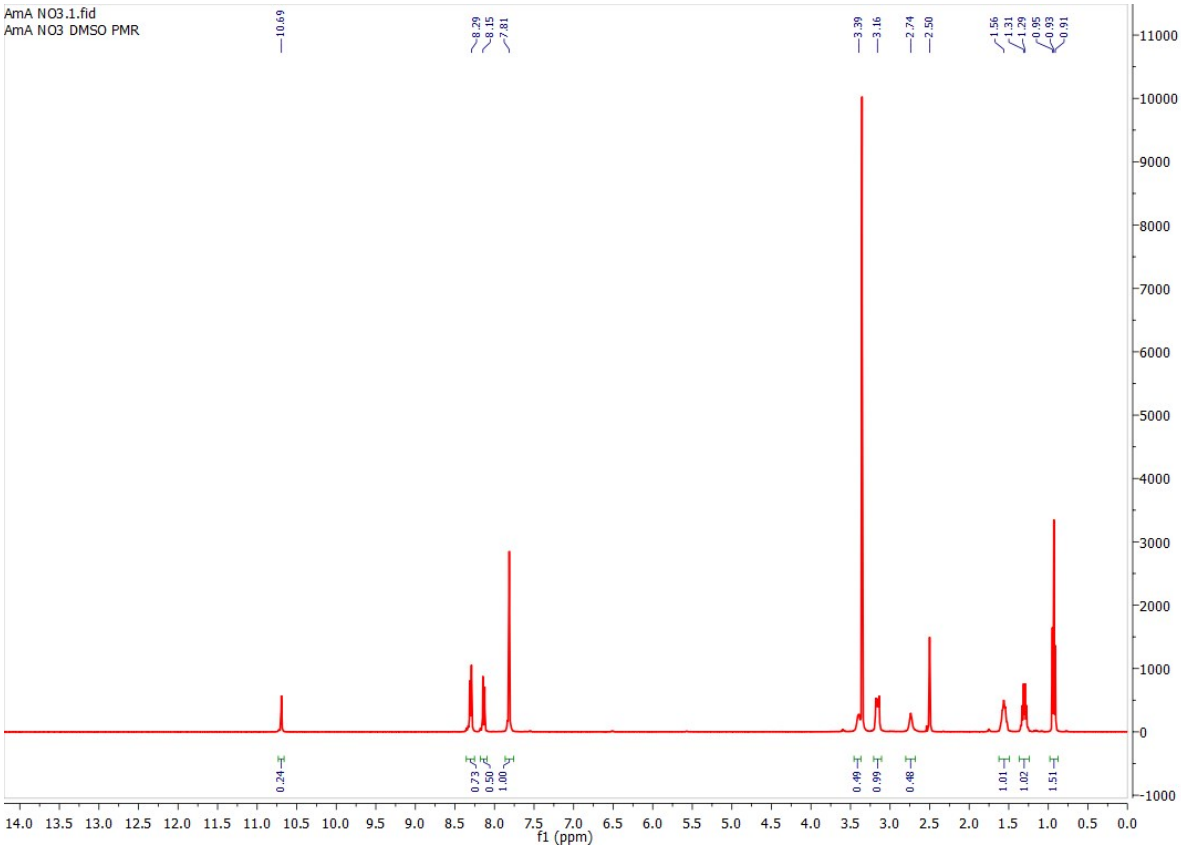

Fig. S39 ^{1}H-NMR spectrum of **AAL** in presence of 2 equivalents of $(n\text{-}Bu_4N^+)NO_3^-$ in DMSO-d_6.

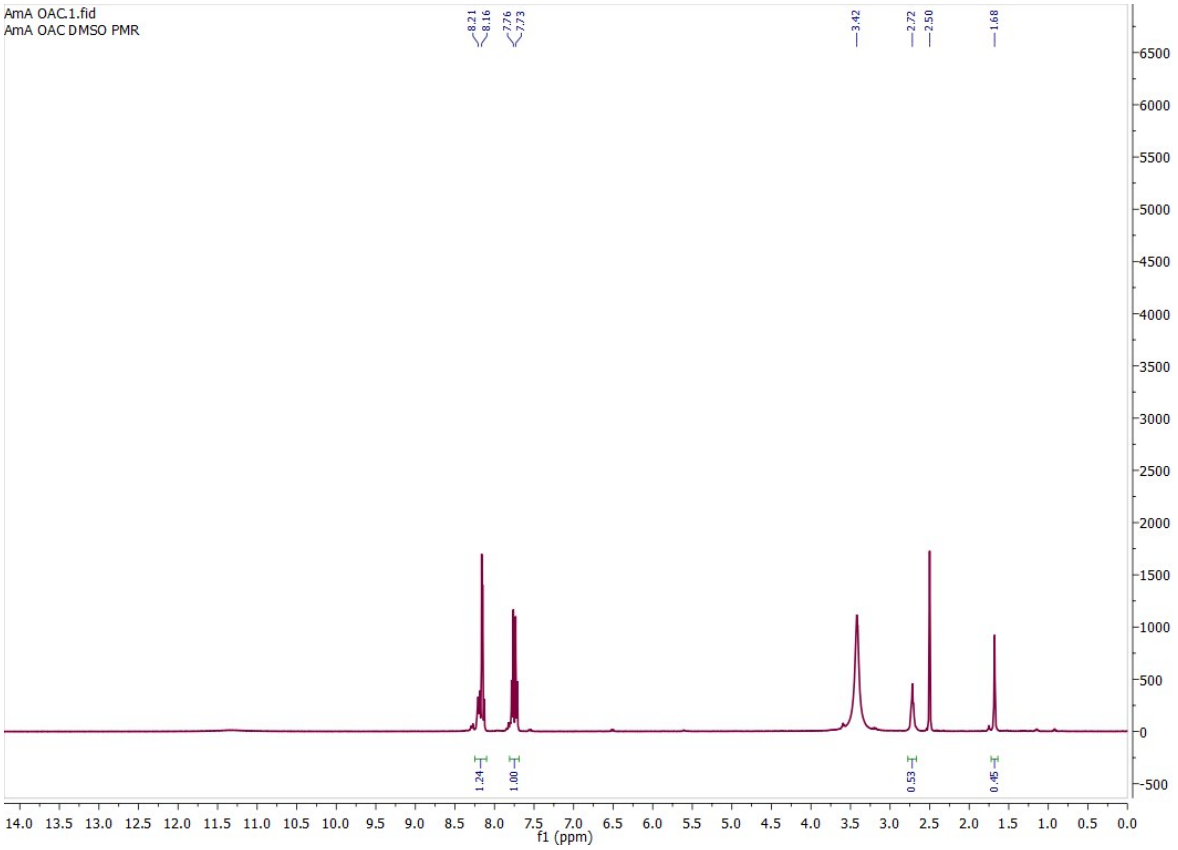

Fig. S40 ^{1}H-NMR spectrum of **AAL** in presence of 2 equivalents of $Li^{+}CH_3COO^{-}$ in DMSO-d_6.

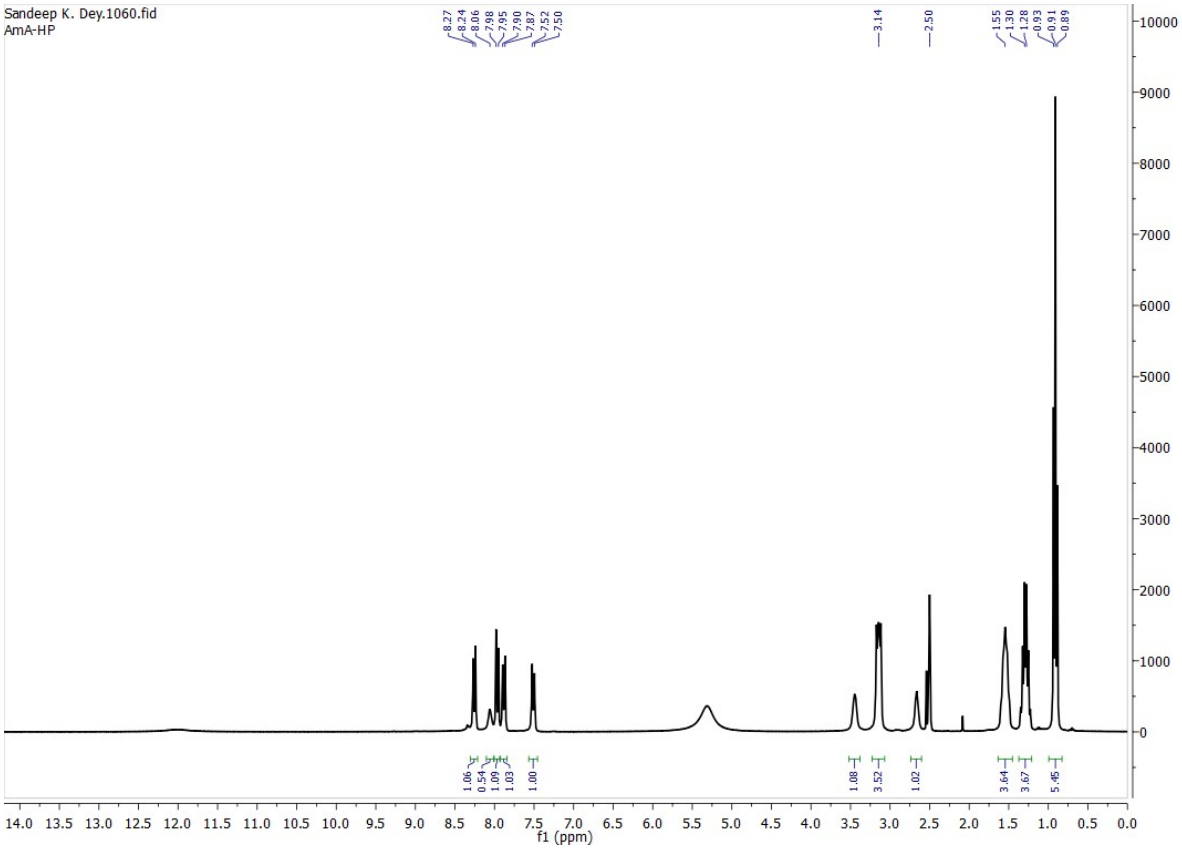

Fig. S41 ^{1}H-NMR spectrum of **AAL** in presence of 3 equivalents of $(n\text{-}Bu_4N^{+})H_2PO_4^{-}$ in DMSO-d_6.

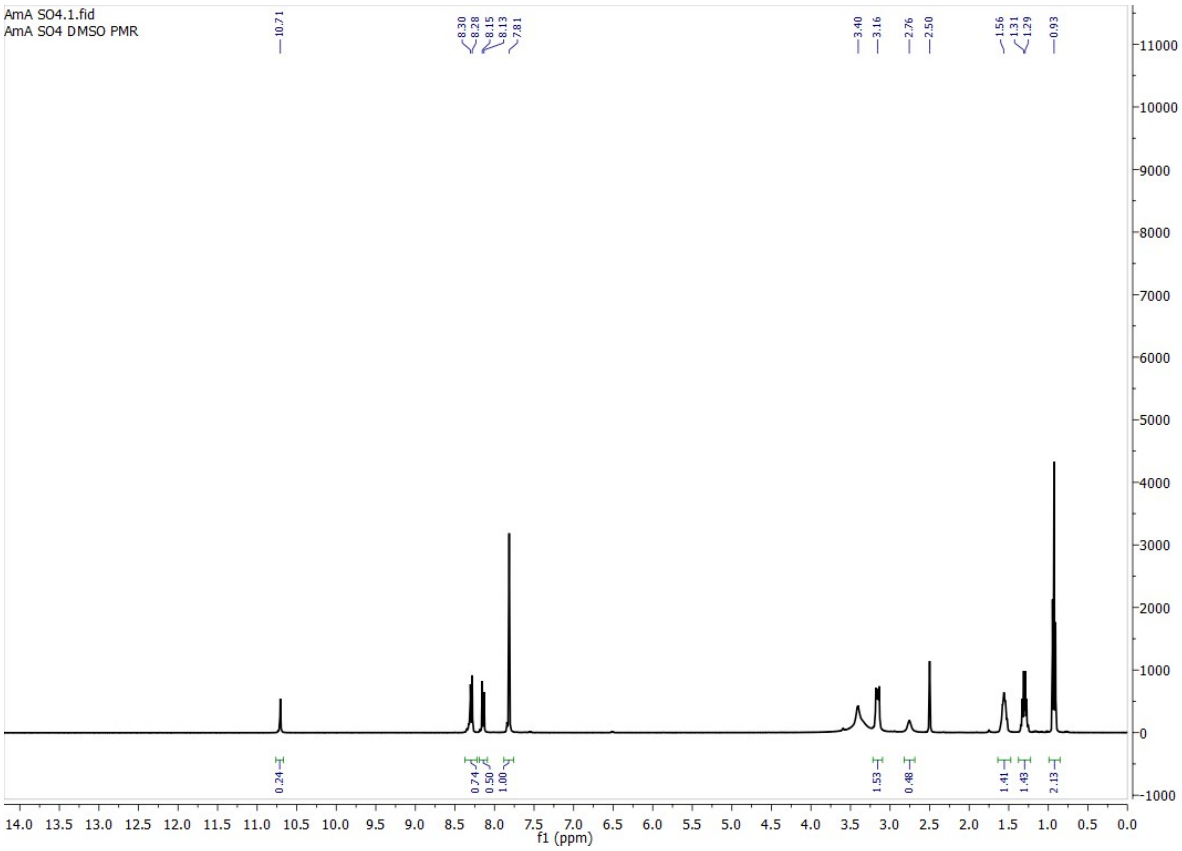

Fig. S42 ^{1}H-NMR spectrum of **AAL** in presence of 2 equivalents of $(n\text{-}Bu_4N^+)HSO_4^-$ in DMSO-d_6.

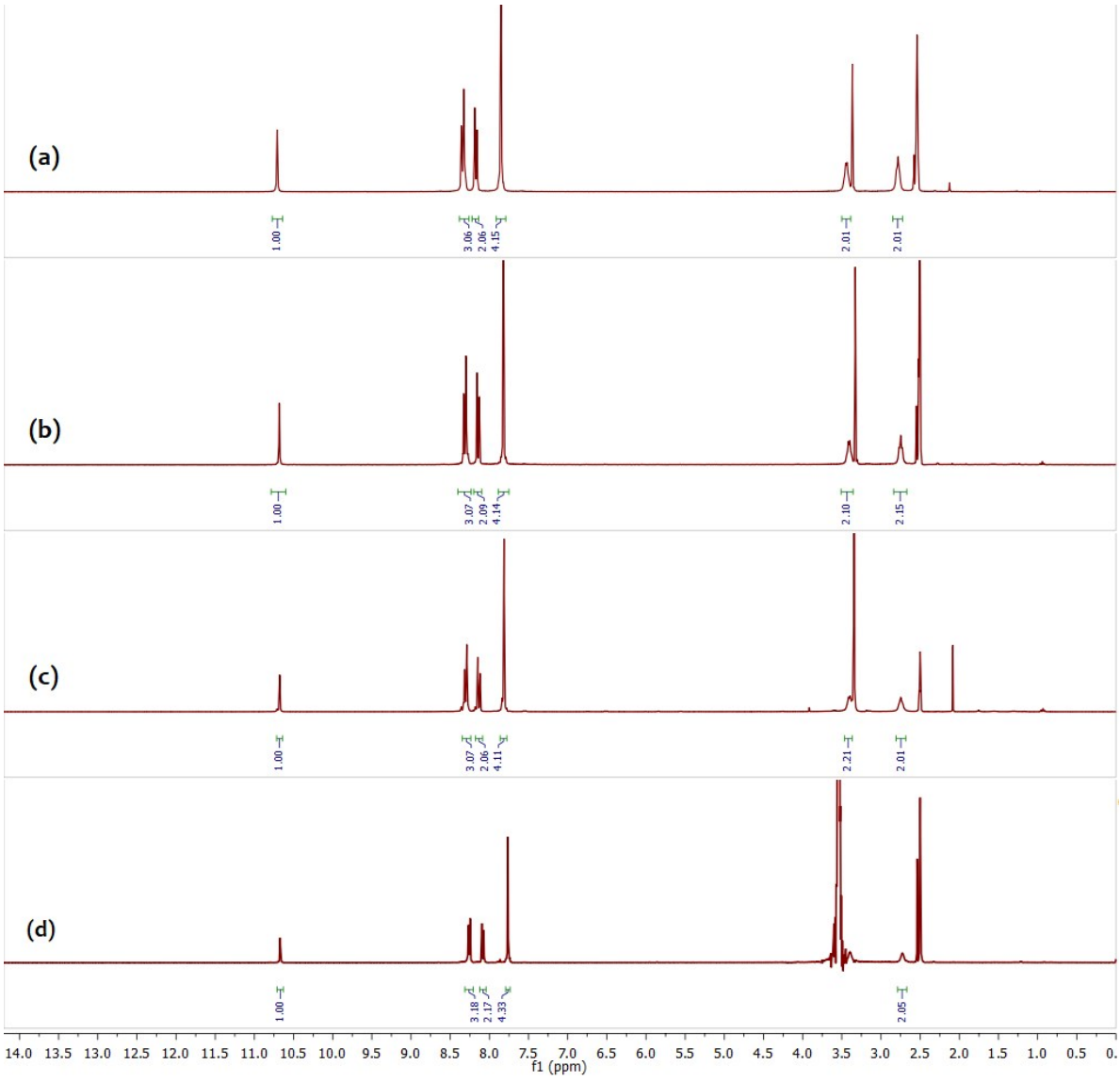

Fig. S43 ^{1}H-NMR spectrum in DMSO-d_6 of (a) **AAL** as synthesized (b) **AAL** precipitate obtained in presence of $(n\text{-}Bu_4N^+)F^-$, (c) **AAL** precipitate obtained in presence of $(Et_4N^+)CN^-$, (d) **AAL** precipitate obtained in presence of $(n\text{-}Bu_4N^+)CH_3COO^-$ from DMSO-CH_3CN solutions in crystallization experiments.

8. Powder X-ray diffraction patterns of AUL and AAL obtained in the presence of quaternary ammonium salts from crystallization experiments at room temperature.

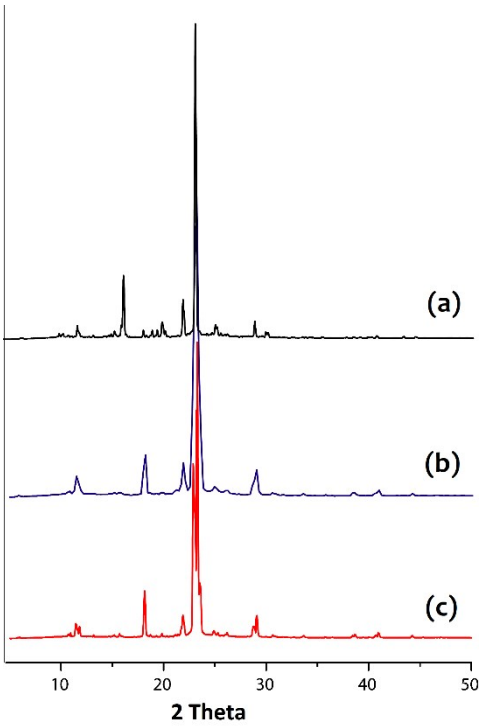

Fig. S44 Powder X-ray diffraction patterns of **AUL** crystals, obtained in the presence of (a) [n-Bu_4N^+]AcO^-, (b) [n-Bu_4N^+]Cl^- and (c) [n-Bu_4N^+]F^- from DMSO/CH_3CN solutions.

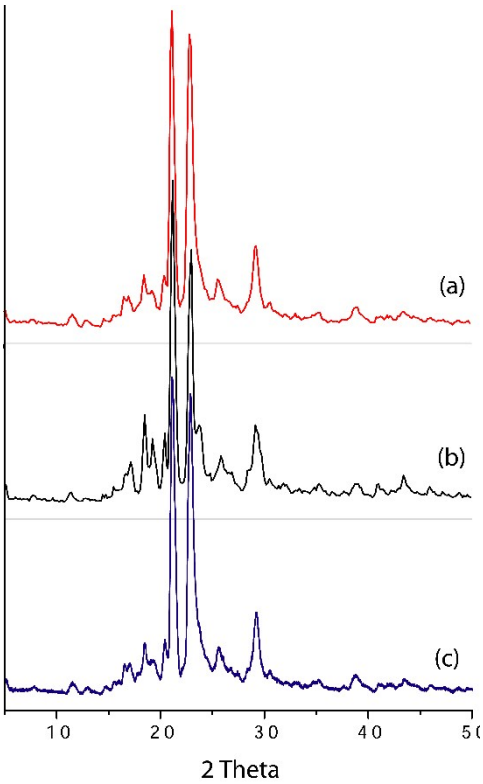

Fig. S45 Powder X-ray diffraction patterns of **AAL**, obtained in the presence of (a) [n-Bu_4N^+]F^-, (b) [n-Bu_4N^+]Cl^- and (c) [n-Bu_4N^+]AcO^- from DMSO/CH_3CN solutions.

9. Single crystal X-ray crystallography

In each case, a crystal of suitable size was selected from the mother liquor and immersed in silicone oil, and it was mounted on to a fibre loop holder and cemented using epoxy resin. Single-crystal XRD data were collected at 296(2) K with a Bruker SMART APEX-III CCD diffractometer equipped with a fine focus 1.75 kW sealed tube Mo–Kα radiation (λ = 0.71073 Å). The SMART software was used for the data acquisition. Data integration and reduction were undertaken with SAINT and XPREP software.[1] Multi-scan empirical absorption corrections were applied to the data using the SADABS program.[2] The structures were solved by direct methods using SHELXS-97,[3] and refined with full-matrix least-squares on F^2 using SHELXL-97.[4] All non-hydrogen atoms were refined anisotropically, hydrogen atoms attached to all carbon atoms were geometrically fixed and the positional and temperature factors were refined isotropically. Hydrogen atoms attached to the amide and urea nitrogen atoms were located from the Electron Fourier map and refined isotropically. In order to model the disorder of a DMSO molecule in **AUL-2DMSO**, a PART-1 command was used and the O-C distances were restricted with DFIX command. The hydrogen atoms on the lattice water molecule in **AL-H_2O** could not be located from the Electron Fourier map or geometrically fixed.

Table S2. Hydrogen bonding contacts (D-H···O) on the encapsulated hydrogenphosphate anion in (n-$Bu_4N)_2$(**AUL**·HPO_4)DMSO·CH_3CN.

D-H···O (HPO_4^{2-})	*d*(H···O)/Å	*d*(D···O)/Å	<D-H···O/°
N3-H···O4	1.990	2.841 (5)	169.8
N4-H···O2	1.960	2.765 (5)	155.5
N7-H···O1	2.117	3.027 (5)	169.3
N8-H···O3	1.938	2.776 (5)	164.6
N11-H···O4	1.976	2.818 (4)	165.6
N12-H···O3	1.851	2.697 (4)	166.9
C12-H···O2	2.957	3.206 (7)	132.8
C32-H···O3	2.746	3.412 (7)	129.4
C44-H···O3	2.637	3.332 (7)	132.1

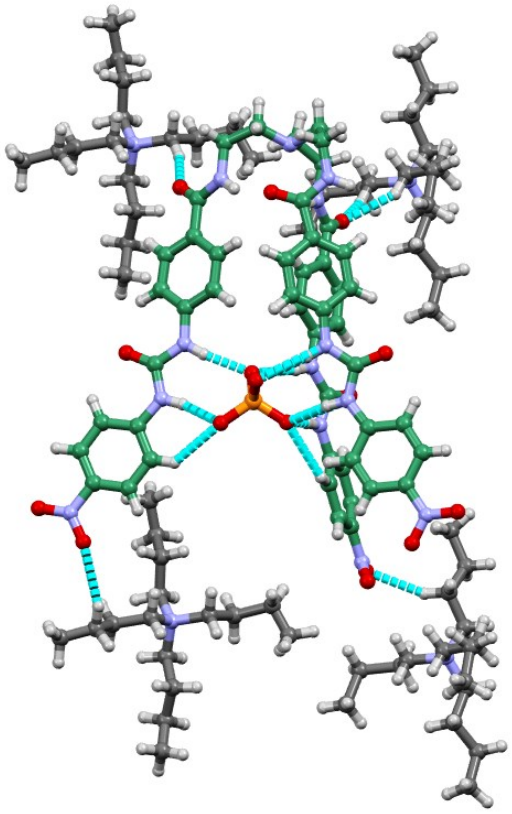

Fig. S46 C-H···O interactions between tetrabutylammonium cations (n-Bu_4N^+) and anion encapsulated **AUL** in [(n-$Bu_4N)_2$(**AUL**·HPO_4)·DMSO·CH_3CN] complex.

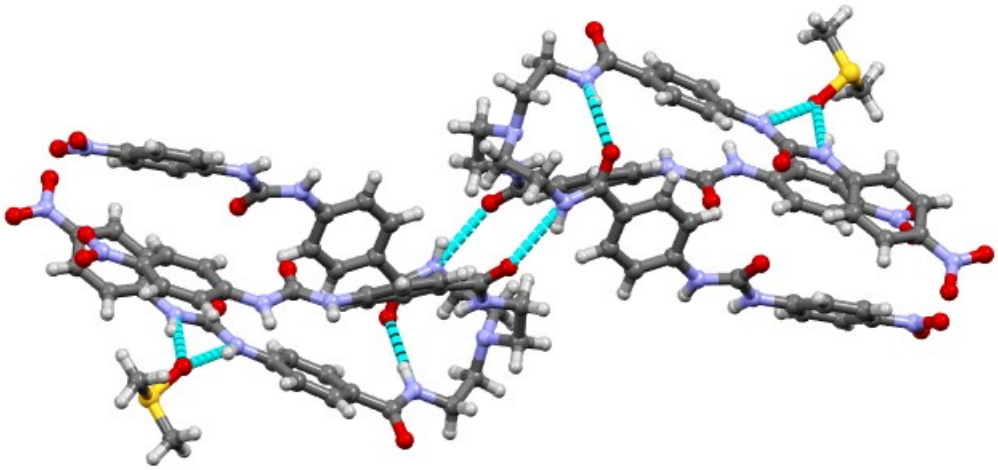

Fig. S47 Intramolecular and intermolecular N-H···O=C hydrogen bonding between the amide groups in **AUL**-2DMSO.

References

1. SMART, SAINT and XPREP, Siemens Analytical X-ray Instruments Inc., Madison, WI, 1995.

2. G. M. Sheldrick, SADABS: Software for Empirical Absorption Correction; University of Gottingen, Institute for Anorganische Chemie de Universitat, Gottingen, Germany, 1999–2003.

3. G. M. Sheldrick, SHELXS-97, University of Gottingen, Germany, 1997.

4. G. M. Sheldrick, SHELXL-97: Program for Crystal Structure Refinement, University of Gottingen, Gottingen, Germany, 1997.